Investigating the Influence of Oxidative Stress and the Role of Prdx1 in the Regulation of Lysyl Oxidase Mediated ECM and Collagen Remodeling in Breast Cancer Metastasis

by

Shireen Attaran

B.S., University of California Davis, 2007

M.S., California State University East Bay, 2013

Submitted to the Graduate Faculty of

School of Medicine in partial fulfillment

of the requirements for the degree of

Doctor of Philosophy

University of Pittsburgh

2018

UNIVERSITY OF PITTSBURGH

SCHOOL OF MEDICINE

This dissertation was presented

by

Shireen Attaran

It was defended on

September 17, 2018

and approved by

Patrick Pagano, Professor, Molecular Pharmacology

Guillermo Romero, Professor, Molecular Pharmacology

Lance Davidson, Professor, Bioengineering

Yi Huang, Assistant Professor, Molecular Pharmacology

Dissertation Director: Carola Neumann, Associate Professor, Molecular Pharmacology

Investigating the Influence of Oxidative Stress and the Role of Prdx1 in the Regulation of Lysyl Oxidase Mediated ECM and Collagen Remodeling in Breast Cancer Metastasis

Shireen Attaran, PhD

University of Pittsburgh, 2018

Breast cancer progression and metastasis includes not only cell-autonomous properties of cancer epithelial cells, but also the influence of the neighboring tumor stromal cells. In breast cancer, almost 80% of stromal associated fibroblasts (SAFs) acquire a cancer associated fibroblast (CAF)-like "activated phenotype". This CAF activated phenotype is associated with elevated levels of reactive oxygen species (ROS) that are linked with tumor remodeling and spreading. Members of the lysyl oxidase (LOX) family of enzymes participate in tumor remodeling through the promotion of collagen crosslinking and collagen fibril production. We hypothesize that stromal Prdx1 regulates ROS dependent metastasis/migration of cancer cells through effects on LOX activity. Our preliminary data reveal that Prdx1 prevents CAF-induced malignant phenotypes in breast cancer (epithelial) cells in an H2O2-dependent manner. When compared to wild-type mice, Prdx1-/- SAFs show a marked increase in CAF-specific characteristics, including increased expression of CAF-specific markers, motility and invasiveness of SAFs and SAF-induced chemotactic migration and invasion by breast cancer epithelial cells in vitro. Lack of Prdx1 in mammary SAFs results in the upregulation of markers of the activated phenotype, such as collagen, vimentin and α-SMA leading to an increase in co-migration and invasion. As shPrdx1 SAFs show CAF-like mesenchymal properties in vitro, we tested in vivo if Prdx1 suppresses migration of breast cancer

cells by generating a syngeneic mouse model to image BALB/c derived SAFs shPrdx1/SAFs pLKO1 (expressing iRFP). Immunoprecipitation data suggests that Prdx1 associates with LOX family proteins. Moreover, Prdx1-deficient SAFs displayed elevated LOX secretion into the ECM compared to Prdx1-proficient SAFs. Lastly, of translational relevance, we have shown that SAF Prdx1 becomes inactivated by cancer cells through phosphorylation of Y194 Prdx1. The peroxidase, Prdx1, is a regulator of LOX and CAF activity and SAFs lacking Prdx1 may serve as a valuable model system to investigate the biology of CAFs in vitro and in vivo.

Table of Contents

List of Tables

List of Figures

Preface

"Human beings are members of a whole, in creation of one essence and soul. If one member is afflicted with pain, other members uneasy will remain. If you have no sympathy for human pain, the name of human you cannot retain"

-Saadi 13th Century Persian Poet

"A ship in harbor is safe, but that is not what ships are built for"

-John A. Shedd

As I reflect on the journey that brought me to this point in my career and life, I have to acknowledge the people who guided and supported me along the way. Without them, I would not be where I am today. First, I would like to thank my thesis advisor, Dr. Carola Neumann, for her unwavering support and guidance as I journeyed through graduate school and developed into a scientist. Thank you for encouraging me at every step along the way. Dr. Patrick Pagano, thank you for recruiting me to Pitt and for your unwavering belief in my potential as a scientist. I want to express my sincere gratitude for the mentorship you provided. Dr. Guillermo Romero, thank you for your mentorship and support. I very much appreciate the insight and expertise you provided to my project. Also, I want to thank the other members of my thesis committee, Dr. Lance Davidson and Dr. Yi Huang—thank you for your insightful feedback and for helping me develop my thesis project. Dr. Adam Feinberg, thank you for your early contributions to my project.

Dr. John Skoko, a very talented post-doc in our lab, thank you for always helping me troubleshoot technical problems and for helping me understand the bigger scientific picture—you have been an amazing colleague and friend and I wish you all the best. The Department of Molecular Pharmacology, especially Dr. Bruce Freeman,

thank you for providing a truly exceptional training program for the graduate students. Also, a very special thank you goes out to the members of the Breast Cancer Research Advocacy Network (bcRAN), thank you for your courage and strength. And, thank you for bringing the human component to breast cancer research and for inspiring me everyday in my research. Also, thank you to Dr. Jose Berrios at the USDA for your constant and unwavering support, mentorship and friendship. You have been instrumental in the development of my career.

I wouldn't have made it this far without the love and support from my friends and family. Nyla, thank you for being an amazing friend—you made my graduate school experience so much fun; I always looked forward to our coffee catch-ups. Gina, thank you for being the best friend a girl could ask for! Even though we were far apart in distance, your friendship always reminded me of the saying, "Good friends are like stars, you don't always see them, but you know they are always there". Thanks for always being there. Also, thank you to my Aunt Elizabeth and Antero, for being so kind to me as a little kid and for always believing I would do big things in my life.

A very special thank you goes to my husband for being my partner in life and for his unwavering love, support and understanding as I ventured thorough the PhD program. I couldn't have done it without you. Thank you for always making me laugh. My daughter, Darya, thank you for coming into our lives when you did! I feel so lucky that the universe chose me to be your mommy. Thank you for inspiring me everyday and for helping me see the beauty in all things. I love you with all my heart.

And, saving the best for last, I want to thank my parents, Mehdi and Gladys, for their unconditional love and support. Thank you for the many sacrifices you made in order to help me realize my dreams. Thank you for always being the most amazing parents and for always making me feel like anything was possible. I would not have made it this far without you and I feel so lucky to be your daughter. Dad, thank you for instilling in me from an early age the importance of education and the value of working hard to achieve your goals. Thank you for your words of wisdom and for always encouraging me and for believing in me no matter what. Thank you for always being my best friend- I couldn't have done this without you. Mom, thank you for teaching me so many things I could never learn in any book or class. Thank you for teaching me to be strong and to fight for what I believe in. Thank you for teaching me to be assertive and to stand up for myself. And also, thank you for showing me how to dream. You both gave me your best qualities and anything I may have accomplished and anything I may have achieved I owe completely to you both. My love for you is endless. I hope I made you proud.

1.0 Introduction

1.1 Breast Cancer

Breast cancer is the most common malignant disease in US women, with over 250,000 new cases and over 70,000 deaths expected in 2018 alone[1]. In these patients, it is not the primary tumor, but rather, the metastases to distant sites in the body that prove fatal[2]. More recently, the rates of mortality due to breast cancer have been declining due to enhanced mammographic screening and adjuvant therapies; however, chemotherapy has a host of both acute and long-term side effects and in some cases, it can even promote metastasis[2, 3]. Novel tools to predict chemotherapeutic benefit personalized to the patient, such as Oncotype DX[4], are just now beginning to emerge; however, to date there are no tools available that can accurately predict which patients will progress to metastatic disease. The four main subtypes of breast cancer are 1) luminal A, 2) luminal B, 3) HER2 overexpressing and 4) triple negative breast cancer[5]. Luminal A breast cancer tends to be slow growing and less aggressive with a high survival rate. It is classified as being ER+, and/or PR+, and HER2-. Luminal B is characterized as being ER+, and/or PR+, and HER2+, with high proliferation rates and a poor prognosis compared to luminal A. HER2 overexpressing cancers tend to grow much more rapidly

and spread more aggressively due to HER2+, ER+ and PR- classifications and lastly, the most aggressive form of the four is triple negative breast cancer, which has the worst prognosis among the four, with higher rates of recurrence after surgery and lack of targeted therapies currently available[5]. Ultimately deaths due to breast cancer are not a result of the primary tumor; instead they are due to the migration of these cancer cells to distant organs in the body, which is why an in-depth understanding of metastasis is critical to designing therapeutics to halt cancer progression and cancer-related deaths.

1.2 Stromal microenvironment in breast cancer

Cancer is a complex and systemic disease, which incorporates numerous components of both tumor and stromal cells embedded within the extracellular matrix (ECM)[6-9]. The microenvironment of a developing tumor is composed of proliferating tumor cells, tumor stroma, angiogenic interactions and immune responses and it is defined as the complex and dynamic interactions between cancer cells and the ECM[10]. Furthermore, tumor associated macrophages (TAMs) play an important role in the secretion of growth factors, angiogenesis, tissue remodeling and the suppression of adaptive immunity. Additionally, bone marrow derived stem cells (BMDSCs); also secrete growth factors that can promote the differentiation of BMDSCs to osteoblasts, fibroblasts, chondrocytes and adipocytes. Primary and metastatic tumors are known to recruit BMDSCs to the microenvironment where they differentiate into tumor-associated fibroblasts, promoting tumor survival and persistence (Figure 1).

Several decades of in-depth cancer research has been focused on a tumor-cell autonomous view of cancer, however, more recently it has become apparent that tumor cells do not act alone, but rather, they persist in a fertile tumor microenvironment which is governed by tumor-stroma interactions to promote metastasis and cancer progression[7, 11-16]. As the cancer continues to evolve, the surrounding tumor stroma and ECM is also transformed into an activated state which is maintained by continuous paracrine signaling between the tumor cells and the host stroma, thereby, cultivating an environment permissive to cancer progression [10, 11].

Fibroblasts were first identified by Virchow and Duvall in 1858, as cells that function to synthesize collagen in connective tissues[17, 18]. Phenotypically, fibroblasts are spindle-shaped, which can become polarized with migratory signaling. In normal tissues, fibroblasts are thought to be in a dormant state because of their relatively low metabolic activity[19]. Quiescent fibroblasts are generally found in the interstitial stromal layers between the parenchyma and mature tissues and they are identified as being long, thin cells with a spindle-like shape[19]. Currently, quiescent cells are defined by their ability to respond to stimuli, such as growth factors, allowing them to become activated, thus prompting proliferation, migration, further production of growth factors and deposition of ECM proteins[11, 19, 20]. Once activated, these fibroblasts display significantly increased contractile and metabolic activity, which are critical components of wound repair and connective tissue production; in cancer, however, these typically normal processes become dysregulated[19].

If there is chronic inflammation or wound insults, either in the context of physical, toxic, autoimmune or metabolic disorders, the repair response will continue unrestricted, resulting in a condition called tissue fibrosis[11, 19, 21]. This process is thought to occur by epigenetic mechanisms

intrinsic to fibroblasts in the activated state, thus enriching anti-apoptotic signals and enhancing proliferation to generate over-activated fibroblasts[19, 20].

In the context of cancer, the tumor stroma is mainly comprised of fibroblasts; many studies to date have established that fibroblasts residing in the tumor microenvironment have a significant influence on cancer progression and invasion[9, 12-14, 16, 22-24]. Fibroblasts in the tumor microenvironment become activated and are termed, cancer associated fibroblasts (CAFs)[13, 21, 25, 26]. Fibroblasts at basal state are typically quiescent; however, they become activated in response to wound healing[20]. Tumors are commonly referred to as wounds that will not heal because of aberrant wound healing responses[27].

Dysregulation of wound healing results from signaling responses which remain elevated and sustained even once the wound is resolved; this is typically observed in tissue fibrosis and tumor progression[20, 27]. CAFs are generally identified by their expression of α-smooth muscle actin (α-SMA), a cytoskeletal protein typically found in smooth muscle cells[19]. The mechanism governing fibroblast activation is still not fully understood; however, it has been shown that reversion of phenotype and behavior of malignant cells can be modified by altering the tumor ECM[28, 29]. This suggested that tumor cells do not act autonomously; rather, they are governed by stromal signaling in the tumor microenvironment.

Early studies in the 1970s described a mechanism by which cancer cells recruit activated fibroblasts that are functionally similar to myofibroblasts associated with wound healing[30, 31]. This recruitment is largely regulated by growth factors secreted by the primary cancer cells and immune cells. TGF-β, PDGF and FGF-2 are the main mediators of activation in fibroblasts in both acute and chronic tissue damage and repair[19]. Furthermore, the recruitment of activated fibroblasts in many cancers is regulated by TGF-β[32]. Moreover, of importance when examining ECM matrix

influences on metastasis, TGF-β, has been shown to increase the activity of lysyl oxidase (LOX), the primary enzyme responsible to collagen crosslinking and remodeling[33]

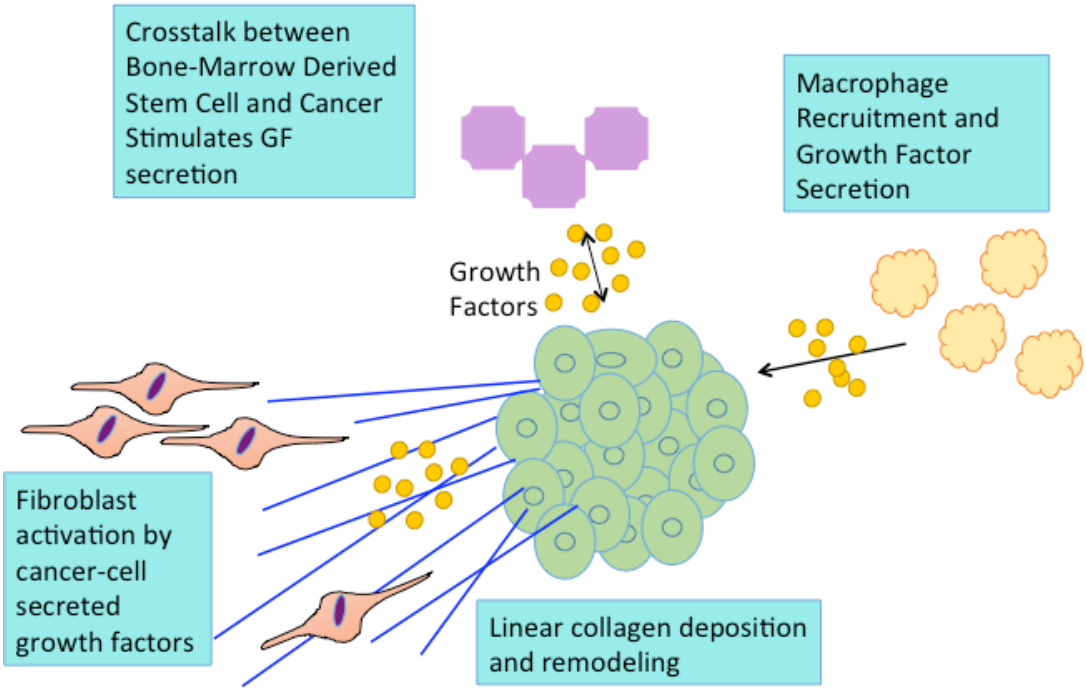

Figure 1 Tumor Microenvrionment The tumor microenvironment is composed of a variety of different factors, which have the primary purpose of sustaining tumor vitality and promoting cancer progression. Bone marrow derived stem cells (BMDSCs) function to secrete growth factors allowing the differentiation into a variety of call types such as fibroblasts, osteoblasts and adipocytes. Macrophages are also recruited to the microenvironment and secrete growth factors that promote cancer progression while also suppressing innate adaptive immune responses. Activated fibroblasts in the microenvironment function to modify the ECM by altering the structure of collagen.

1.2.1 Lysyl Oxidase and Implications in Cancer

Lysyl oxidase (LOX) and its family members, the LOX-like protein LOXL1-4 are copper dependent amine oxidases, which function to oxidize the ε-amino group of the peptidyl lysine to peptidyl aldehydes, subsequently followed by formation of dehydrolysinonorleucine and aldol condensation products from peptidyl aldehydes and lysine residues[34, 35]. Essentially, they are ECM enzymes, which function to catalyze collagen crosslinking in the stroma of the ECM, thus directly influencing the tensile strength of tissues[36]. All five of the LOX family members are highly conserved at the C-terminal catalytic domain; this includes the copper binding site, the lysyl tyrosyl quinine domain (LTQ) and the cytokine receptor like domain (CRL) (Figure 2). The copper and LTQ domains are absolutely essential to the oxidase activity of the LOX family member enxymes[35, 37, 38]. Copper is not directly involved with the catalytic component of LOX, however, it is crucial for maintenance of the LTQ domain and the conformation of the LOX protein[34].

The LTQ domain functions to maintain a negative charge in the LTQ pocket promoting copper recruitment; the LTQ domain is covalently linked via K314 and Y349 residues[36]. The LOX family members have significant differences on the N-terminus; LOXL1 contains a proline-rich domain and LOXL2, LOXL3 and LOXL4 contain four scavenging receptor cysteine-rich domains (SRCR)[36]. The SRCR region is frequently found at the cell surface and is thought to be involved in protein-protein interactions. The LOX family members are synthesized as zymogens in the endoplasmic reticulum. The pro-peptides are secreted into the ECM and the NH_2-terminal pro-peptide of LOX is cleaved by bone morphogenic protein-1 (BMP-1), thus allowing for enzyme activation and functioning oxidase activity[35, 36]

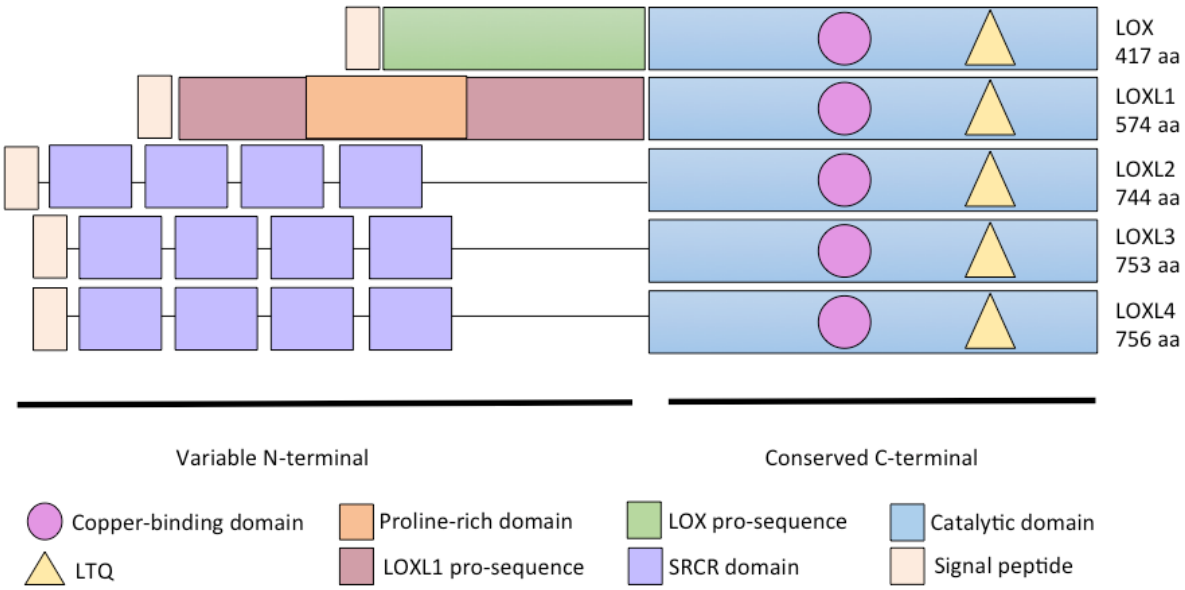

Figure 2 LOX Family Domains All members of the LOX family have a conserved C-terminal domain, which contains the catalytic domain responsible for providing the enzymatic crosslinking activity of the enzyme. Differences in family members can be seen on the N-terminal domain. LOXL2-LOXL4 all contain a scavenging receptor cysteine-rich (SRCR) domain. LOX and LOXL1 contain a pro-sequence domain.

Once in the extracellular space and cleaved by BMP-1, LOX is in its active form and it can participate and catalyze crosslinking events of ECM protein such as collagen and elastin. These crosslinking reactions catalyzed by LOX provide tensile strength and integrity to connective tissues and also participate in wound repair cascades[35, 39]. Meticulous regulation of expression and activity of LOX is critical to sustaining tissue homeostasis. When dysregulation of LOX occurs, the pathogenesis of diseases such as tissue fibrosis and cancer arise[35]. LOX is regulated by a variety of pathways including transcriptional regulation and both temporal and spatial distributions, thereby modulating enzyme activity[34].

A critical cytokine responsible for regulating the ECM is TGF-β; it functions by regulating both ECM structural protein expression and via direct influences on ECM remodeling enzymes

such as LOX[34, 35]. TGF-β has been shown to increase LOX mRNA expression in a time and dose-dependent fashion via PI3K and MAPK signaling[40]. In cardiac fibrosis, it has been shown that high doses of TNF-α results in LOX expression, causing an increase in collagen crosslinking and leading to an elevation in detrimental fibrosis[41].

LOX function is of critical importance to maintain normal homeostasis. Mice lacking LOX were described to be perinatal lethal, exhibiting ruptured diaphragms, arterial aneurysms, and disjointed elastic fibers[42]. The two most widely studied genetic diseases of copper metabolism are Menke's and Wilson's disease, which present with strikingly low levels of LOX activity due to the consequence of copper deficiency[43]. In these conditions, there is a marked decrease in fiber elasticity resulting in weakening of the structural integrity of tissues[43]. In a striking contrast, LOX activity is markedly upregulated in atherosclerosis, liver cirrhosis, and schleroderma[44, 45].

LOX is widely accepted as a poor prognosis factor, specifically in promoting metastasis in breast cancer[34, 46], head and neck squamous cell carcinoma[47] and lung[48] and prostate cancer[16] (Table 1). In the context of breast cancer, it is important to understand that increased expression of LOX has been observed in invasive basal breast cancer, however, this elevation of LOX is not observed in non-invasive breast cancers[49]. Normal development in the mammary gland is mediated via GATA-3, a transcription factor that regulates differentiation of luminal cells and also negatively regulates LOX via methylation of the LOX promoter[49]. Furthermore, the transcription factor forkhead box M1b (FOXM1b), directly binds to the promoter of both LOX and LOXL2, leading to increased expression and activating the Akt/SNAIL pathway, leading to an elevation in liver fibrosis and metastasis of hepatocellular carcinoma; FOXM1b is overexpressed in human cancers and is correlated with poor prognosis[49]. Another critical regulator of LOX expression is

dependent upon hypoxia. In conditions of hypoxia, LOX mRNA is significantly upregulated via the transcription factor HIF1α[47].

The biomechanical properties of the tumor microenvironment have a critical role and influence on the behavior of cells residing in the microenvironment and there is a significant body of evidence highlighting the importance of collagen as the primary protein governing the mechanical component of the microenvironment[37, 50-53]. Recent studies have suggested that increased ECM protein deposition resulting in elevated tissue stiffness, steers cancer progression to metastasis, primarily via actinomyosin and cytoskeletal rearrangements, cellular contractions and altered growth factor signaling[37, 51-54]. To date, the mechanism behind this phenomenon has not yet been completely elucidated; however, more evidence has emerged suggesting that collagen crosslinking by the LOX family members have a critical role in supporting and promoting metastatic disease[37, 52, 53, 55, 56].

Cancer	Family	Role	Ref.
Breast	LOX	Increased expression correlated with increased metastasis and overall poor prognosis	57-59
	LOXL2	Increased expression in tumor stroma compared to normal stroma	48, 60-62
Colorectal	LOX	Increased expression= increased invasion, metastasis and SRC activation	63, 64
	LOXL2	Increased expression in tumor stroma	64
Lung	LOXL2	Increased expression= Poor prognosis	48
Hepatocellular	LOXL2	Increased expression in tumor stroma	65
Basal and squamous skin cell carcinoma	LOX	Decreased expression= increased invasiveness	66
Pancreatic	LOXL2	Increased expression in tumor stroma	67, 68
Laryngeal	LOXL2	Increased expression in tumor stroma	69

Table 1. LOX Family Members and Role in Cancers

1.2.2 Collagen Remodeling and Implications in Breast Cancer Metastasis

Collagen is the most abundant protein in the body, representing approximately 30% of total mammalian protein mass and roughly 28 different forms of collagen have been identified in vertebrates[70, 71]. The primary structural component of the interstitial ECM is Type-I collagen, while in the basement membrane, Type IV collagen predominates playing a critical role in tissue polarity[72]. Collagen, being a fibrous protein which provides structural integrity to tissues, is composed of three polypeptide α-chains held together by hydrogen bonding, containing a polyproline, to form a right handed supercoil conformation[73]. The collagen triple helix provides a molecular conformation, which grants rigorous requirements of the amino acid sequence, demanding a Gly-X-Y repeating pattern[73].

Collagen endures vast post-translational modifications by crosslinking and hydroxylation reactions in the endoplasmic reticulum before the triple helix is formed. A wide variety of chaperones and enzymes assist the proper trimerization and folding of collagen[73]. Depending upon the structural properties of the ECM, collagen can form classic fibrillar fibers or network-forming collagens[71]. Among the many forms of collagen, collagen-I is the model fiber because its triple helix has no imperfections and it can self assemble into fibrils, while other variants of collagen cannot[74].

Under normal conditions of development such as branching morphogenesis of mammary ducts, epithelial cells interact with collagens in the ECM while also invading the basement membrane to pursue mammary gland expansion[75]. The same mechanism occurs in cancer cell progression, but in an aberrant and unregulated fashion. In many malignancies, desmoplasia is observed; this is defined as a robust fibrotic reaction characterized by a sustained deposition of fibrillar collagen I and III with an increased degradation of collagen IV[19, 20, 56]. In the setting of

breast cancer, increased incidence of these fibrillar collagens is correlated with poor prognosis; desmoplasia has been identified at metastatic sites functioning to support the successful establishment of metastases[52, 56].

In cancer, the structural integrity of the ECM withstands significant alterations during tumorigenesis, such as increased matrix cross-linking, deposition of fibronectin, proteoglycans and collagens I, III and IV. This progressive remodeling, which occurs during tumor evolution, creates a new, reorganized environment permissive to cancer progression by enabling the dysregulation of cell polarity, cell-cell adhesions and enhancing growth factor signaling[76, 77]. Furthermore, this architectural remodeling of the ECM results in morphological changes illustrated by the transformation of normal, curly collagen fibers to the formation of linearized interstitial collagen fibers at the invasion front of tumor progression[77].

In breast cancer, it has been long established that there is an important connection between cancer risk and breast density[78]. In normal, healthy epithelial tissues, the surrounding collagen is phenotypically curly and anisotropic. In progressive cancer, however, the collagen fibers undergo dramatic structural alterations; collagen fibers are transformed to linear, stiff fibers. This structural modification of collagen is ideal for the promotion of metastasis because it fosters the migration of tumor cells to the ECM[51, 52, 54, 79]. In a study conducted investigating the migratory patterns of breast cancer cells, intravital imaging showed that breast cancer cells and leukocytes do undeniably migrate along linearized collagen fiber highways[80]. More recently, better tools have been developed to characterize and classify architectural modifications in the ECM. Tumor associated collagen signatures (TACS) have been characterized to better define ECM architectural changes that occur in tumor progression. Using mouse models of breast cancer, initial changes in ECM architecture were observed as a localized increase of collagen deposition surrounding the tumor

border; this is termed TACS-1. As the tumor continues to grow and evolve, linearized collagen fibers begin to form tangent to the tumor border; this is defined as TACS-2. As reorganization of the ECM progresses even further, the linear collagen fibers begin reorienting perpendicular to the tumor border; this is termed TACS-3[54]. Further supporting these collagen signatures, studies conducted in the context of invasive breast cancer have shown that collagen is modified from a curly, anisotropic fiber to a stiff linear fiber. Moreover, at the invasive tumor border, linearized collagen fibers, perpendicular to the tumor edge can be visualized, further supporting the validity of TACS[52-54, 81].

1.3 Reactive oxygen species and Peroxiredoxin 1

Reduction and oxidation (redox) chemistry is defined by reactions in which reduction causes a gain of electrons, while oxidation is represented by a loss of electrons. In biological systems, redox reactions can regulate intracellular levels of reactive oxygen (ROS) and nitrogen species (RNS) to control a multitude of intracellular processes. These reactive species include both radical and non-radical forms of ROS and RNS such as superoxide anion ($O2^{\bullet}$), hydrogen peroxide (H_2O_2), hydroxyl radical ($^{\bullet}OH$), nitric oxide ($NO^{\bullet}$), nitrogen dioxide ($NO_2^{\bullet}$) and peroxynitrite (ONOO). The relative reactivity of these species spans several log orders of magnitude to affect the half-life and distance traveled within the intracellular environment. The hydroxyl radical is the most reactive species with a half-life on the order of 10^{-9} s, while H_2O_2 is much less reactive in comparison with a half-life of 10^{-3} s[82]. Many of these reactive species were initially regarded primarily as deleterious oxidants due to the recognition that an overabundance of ROS and RNS cause damage to DNA, proteins, lipids and carbohydrates. ROS and RNS were therefore thought

to require reduction to more inert forms in order to maintain intracellular homeostasis and prevent pathophysiological damage. Further research has indicated that ROS and RNS play more complex roles in the cell with mounting evidence supporting a role for these species as mediators at lower concentrations to control protein function and coordinate cell-signaling pathways.

There are diverse sources of ROS that emerge from several organelles within the cell. The intracellular concentration of H_2O_2 has been estimated to be on the order of 1 to 10 nM[83] under basal conditions and reach 0.5 to 0.7 μM during oxidative signaling[84]. Mitochondria have been suggested to be a primary source of ROS due to the byproducts of oxidative phosphorylation to produce ATP. H_2O_2 production has been determined to arise from as much as 1-2% of the total oxygen utilized in isolated rat liver mitochondria during respiration[85], but there is debate as to the magnitude[86] and the concentration of H_2O_2 produced *in vivo*[87]. Complex I[88, 89] and III[90] produce a large proportion of the ROS generated within the mitochondria as $O_2^{\bullet}$[91], which is then reduced to H_2O_2 through catalytic dismutation by Mn-SOD[92]. The steady-state levels of $O_2^{\bullet}$ have been suggested to be relatively low[87] based on the enzymatic reaction rate ($k = 10^9\ M^{-1}\cdot s^{-1}$)[93] and mitochondrial concentrations of MnSOD, which have been measured to be more than 10 μM in isolated rat liver mitochondria[94]. Other organelles that produce ROS include peroxisomes[95] the endoplasmic reticulum[85, 96] and lysosomes[97]. The plasma membrane and cytoplasm also produce ROS through the action of NADPH oxidase[98], prostaglandin synthase[99] , lipoxygenases[100] and xanthine oxidase[101] and transition metals[102], respectively. All of these sources contribute to both the intracellular H_2O_2 load as well as the extracellular secretion of H_2O_2, which can reach 2 μM in stimulated neutrophils[103].

H_2O_2 is recognized as a particularly important reactive molecule with second messenger function. Spatiotemporal features of the molecule enable it to possess reactivity, yet move through

biological macromolecular microenvironments intracellularly within different organelle compartments and intercellularly to neighboring cells. Organ and cellular systems coordinate the balance of the H_2O_2 through enzymatic-catalyzed reductant proteins in conjunction with the pro-oxidant sources mentioned above to form an interconnected network that maintains homeostasis or drives oxidative signaling. The enzymatic metabolism of H_2O_2 is primarily catalyzed through the action of catalase, glutathione peroxidases (GPx) and peroxiredoxins (Prdx). While all three enzymatically metabolize H_2O_2, important biochemical and biological differences exist. Insight into the basal function of the three enzymes *in vivo* can be drawn from the phenotypic effects observed in gene knockout studies. Deletion of catalase or GPx1 display no overt phenotypic changes under basal conditions in mice[104, 105]. This contrasts with the pathophysiological changes that exist upon deletion of Prdx1. Prdx1 knockout mice exhibit increased oxidative damage to DNA and cancer incidence at various sites throughout the animal as well as shortened lifespan and hemolytic anemia[106]. Deletion of the yeast Prdx homolog tsa1 has also been shown to have deleterious effects such as increased oxidative damage, thermosensitivity, mutagenesis and genomic instability[107, 108].

Catalase is localized within peroxisomes and catalyzes decomposition of H_2O_2 via an iron heme porphyrin complex[109]. Sequestration of catalase to a single organelle enables control of peroxisomal H_2O_2 levels, but also requires H_2O_2 derived from other intra and extracellular sources to diffuse to the peroxisome in order for catalase-dependent catalysis to occur. Catalase exhibits a high H_2O_2 turnover rate[110], but sequestration in combination with other enzyme kinetic properties, such as a K_m close to 100 mM in human erythrocytes[110], yield an enzyme that is less effective when H_2O_2 concentrations are low. Contrasting catalase, GPx family members are not present in one organelle. There are eight family members in the glutathione peroxidases (GPx) family (GPx1-

8). GPx1-4 utilize a selenocysteine active site and glutathione (GSH) as a co-factor to reduce H_2O_2[111, 112]. GPx1 and 4 are present in most tissues, with GPx1 expression found in the cytoplasm and mitochondria and the phospholipid hydroperoxide reducing GPx4 is found in the plasma membrane and cytoplasm[112]. Although GPx1 and 4 don't display true Michaelis Menten kinetics, the second order rate constant of the two-part catalytic cycle is in the range of 10^5 M^{-1} s^{-1} [112].

The Prdx family has 6 members (Prdx1-6) that are present in many cellular compartments. Prdx1, 2 and 6 are located in the cytoplasm and nucleus; Prdx3 is localized to the mitochondria; Prdx4 is found in the endoplasmic reticulum; and Prdx5 is located in the peroxisomes, cytoplasm and mitochondria[113]. The Prdx family have 1 or 2-cysteine (Cys)-dependent reaction mechanisms to reduce H_2O_2 to water. The family is subdivided into groups classified as 2-Cys (Prdx1-4), atypical 2-Cys (Prdx5) and 1-Cys (Prdx6) isoforms based on their structure and mechanism of action[114]. The active site peroxidatic Cys is conserved among all family members at roughly 50 amino acids from the N-terminus. The peroxidatic Cys is highly reactive to H_2O_2 due to surrounding amino acids with rate constants on the order of 10^6 to 10^8 M^{-1} s^{-1} [115]. Homodimerization of Prdx proteins in a N-terminus head to C-terminus tail fashion enables 2-Cys family members to align the peroxidatic Cys to the mechanistically important resolving Cys located on the opposing Prdx homodimerization partner near the C-terminus. Prdx1 and 2 homodimers can associate non-covalently to form larger decameric complexes that is ordered as a pentamer of dimers to form a doughnut-like structure[116, 117]. In 2-Cys Prdx, the peroxidatic Cys is oxidized by H_2O_2 to a sulfenic acid moiety, which then forms a disulfide bond with the resolving Cys on the homodimerization partner[118, 119](Figure 2). The disulfide bound dimer destabilizes decameric Prdx to cause dissociation of the complex[120, 121]. The redox reaction cycle can be regenerated by reducing the formed homodimer disulfide bond with thioredoxin (Trx)[117]. The

peroxidatic Cys can become overwhelmed in the presence of high levels of H_2O_2 and become overoxidized to form Cys sulfinic or further sulfonic moieties that lack peroxidase activity. The rate constant of the sulfenic acid form of Prdx2 with H_2O_2 to form the sulfinic Prdx is on the order of 10^4 M^{-1} s^{-1}[122]. The sulfinic form was found to be reversible via enzymatic reduction by sulfiredoxin protein[123]. In addition to the classic Trx recycling, a second redox cycle has recently been described for Prdx2. The sulfenic peroxidatic Cys can be adducted with GSH (rate constant 500 M^{-1} s^{-1}) under physiological concentrations to protect from overoxidation and recycle with Grx1[124]. The atypical Prdx5 follows a similar reaction mechanism, but contrasts typical 2-Cys Prdx by forming an intramolecular disulfide bond with the resolving Cys as opposed to an intermolecular disulfide bond[125, 126]. The 1-Cys Prdx6 protein still forms homodimers, but does not form a disulfide bond following oxidation of the peroxidatic Cys and instead exists in the sulfenic acid form that is reduced with GSH[127].

The peroxidase activity of 2-Cys Prdx has been tied to redox sensor functions to control cell signaling pathways through protein coupling reactions[128]. Prdx2 has recently been shown to participate in a thiol disulfide exchange reaction with the transcription factor STAT3 to repress transcriptional activation[129]. The highly sensitive peroxidatic Cys of Prdx2 therefore acts akin to an oxidative receptor that transfers the oxidative signaling equivalents to a partnering target protein through a Cys redox relay. This mechanism enables the coordination of oxidative signaling to target proteins in the absence of high concentrations of H_2O_2 or highly reactive Cys elements in target proteins. Redox relays exist within the cytoplasm for Prdx1[130]and have been further investigated in larger scale studies. CRISPR-Cas9 deletion of the cytoplasmic Prdx family members Prdx1 and 2 in HAP1 cells showed that cells without Prdx1 or 2 had less oxidation of cytoplasmic protein thiols globally and further support the importance of the redox relay

hypothesis[131]. Other cellular compartments also show redox relay actions such as the ER for Prdx4[132] and Gpx7[133]. This mechanism is currently under further exploration to resolve how many proteins, labeled as redox regulated, undergo oxidation with rate constants on the order of 10 to 10^2 M^{-1} s^{-1}[134] outside of close proximity to an H_2O_2 generating source within a cellular environment with abundant highly reactive peroxidases.

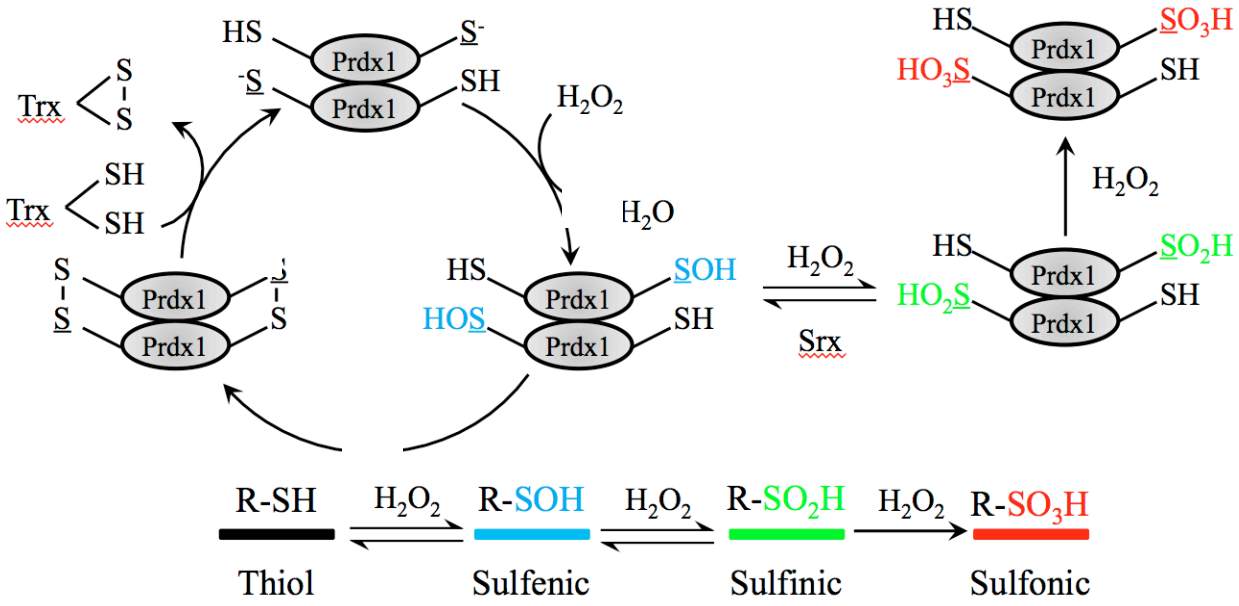

Figure 3. Reduction of H_2O_2 by Prdx1 Peroxiredoxins (Prdxs) are a family of small (22–27 kDa) non-seleno peroxidases currently known to possess six mammalian isoforms. Although their individual roles in cellular redox regulation and antioxidant protection are quite distinct, they all catalyze peroxide reduction of H_2O_2 (1st step of cycle). In the 2nd step of the cycle, resolution of sulfenic acid is where they all differ. Prdx1 & 2 both have catalytic Cys 52 and resolving cysteine, Cys 173. In the 3rd step of the cycle, Trx, regenerates the redox reaction cycle by reducing the homodimer disulfide bond.

Outside of oxidation of the peroW2wzzxidatic Cys in Prdx proteins other factors have been described to alter peroxidase activity and structure including local microenvironmental aspects such as pH[135], ionic strength[136], and temperature[137]. Post-translational modifications can affect peroxidase activity and structure and cell signaling coordination of Prdx activity is apparent through phosphorylation at different sites within the protein. Phosphorylation of Prdx1 to modulate structure and function are seen on Ser32, Thr90, Thr183 and Tyr194. A classic counter-example to the redox relay supported cell signaling coordination by Prdx described above is provided by phosphorylation of Tyr194 on Prdx1 by Src[138]. Local inactivation of Prdx1 peroxidase activity generates increased zonal concentrations of H_2O_2 through the action of Nox[139] at the plasma membrane that is required to drive growth factor receptor tyrosine kinase signaling[140, 141]. Phosphorylation on Tyr194 in response to treatment of cells with EGF or PDGF displayed isoform selectivity for Prdx1 in comparison to Prdx2. Studies showed that siRNA knockdown or pharmacological inhibition of Src reduced the phosphorylation. The peroxidatic Cys was protected from overoxidation of phosphorylation protein during co-treatment of cells with growth factor and H_2O_2. *In vitro* studies of the phosphorylated protein found the dimeric form of the Prdx1 was present without decamers. I*n vivo* wound healing experiments found that Tyr194 phosphorylation peaked after 1 day and remained for 1 week.

Local H_2O_2 accumulation through inactivation of Prdx1 by phosphorylation is also important in the nucleus during mitosis[142]. During early mitosis Prdx1 bound to the centrosome is inactivated by Cdk1-cyclinB phosphorylation of Prdx1 at Thr90 to promote inactivation of the dual-specificity protein tyrosine phosphatase Cdc14B by elevated H_2O_2[143]. Inactivation of Cdc14B and possibly other mitotic exit phosphatases sensitive to inactivation by H_2O_2, enables active Cdk1-cyclin B to transition cells to late mitosis where Prdx1 can be dephosphorylated to promote

deactivation of Cdk1 via dephosphorylation by the now activated Cdc14B. The importance of centrosomal H_2O_2 during the transition to mitosis was evaluated by expressing catalase fused to a centrosomal targeting sequence, which inhibited entry into mitosis. Phosphorylation of the Thr90 residue of Prdx1 by the kinase Mst1 and possibly Mst2 has also been described[144]. Mst1 in the full-length form is localized in the cytoplasm, but caspase cleavage causes nuclear translocation of the kinase[145], whether Mst1 inactivation of Prdx1 is cell compartment generalized or specific to the nucleus or cytoplasm is unknown. Mst1 can additionally phosphorylate Thr183 in the C-terminus of the Prdx1, which was shown to also inactivate peroxidase activity *in vitro* using site-directed mutagenesis to yield Prdx1 Thr183Asp purified protein[144]. Expression of mutant Prdx1 Cys183Asp protein in *Prdx1*$^{-/-}$ mouse embryonic fibroblasts (MEFs) showed heightened levels of the DNA damage biomarker phosphorylated Ser139 H2AX following treatment with H_2O_2. The inactivation of Prdx1 by Mst1 could potentially cause a positive feedback loop whereby excess H_2O_2 further activates Mst1.

Phosphorylation is not only repressive of Prdx1 peroxidase activity. The T-cell-originated protein kinase (TOPK) can phosphorylate Prdx1 on Ser32 to enhance peroxidase activity (20647304). During a mass spectrometry investigation into proteins that bind TOPK in response to ultraviolet light B irradiation of RPMI7951 cells, Prdx1 was identified and following phosphorylation found to have reduced accumulation if H_2O_2 *in vitro* and *ex vivo*. In the absence of TOPK via siRNA decrease, cells were more sensitive to UVB-induced apoptosis. Melanoma cells expressing wild-type, but not Ser32Ala Prdx mutant, protein were more resistant to UVB irradiation. Whether Prdx2 can also be phosphorylated by TOPK is unknown, but may not be seen in experiments with RPMI7951 cells, which only express high levels of Prdx1.

As Prdx1 is not typically mutated in cancers (Table 2), it is critical to investigate the importance of post-translational modifications in the context of cancer. Phosphorylation of Prdx1 on Y194 has been described in the context of wound healing[138]. Prdx1 associated with the cell membrane is transiently phosphorylated on Y194, thereby becoming inactivated in cells stimulated by growth factors or immune responses *in vitro* and at the margins of wound healing at cutaneous lesions in mice. This transient accumulation of H_2O_2 around cell membranes, where signaling components are concentrated, allows for localized inactivation of Prdx1 allowing H_2O_2-dependent signaling to take place without risking toxic accumulation of H_2O_2 at other sites where signaling components are absent, risking toxicity[138]. Moreover, in an analysis of clinical biosets, Prdx1 expression was found to be higher in tumor-associated stroma compared to both normal epithelium and normal stroma (Table 3).

Cancer Type	Cases	Mutation rate (%) PRDX1-6	Deletion rate (%) PRDX1-6
Breast	816	1	0.4
Ovarian	311	0	1.6
Lung	178	3.4	0.6
Bladder	127	7.1	0
Liver	366	1.6	1.1
Head and Neck	279	0.7	2.9

Table 2. Comparison of mutation and deletion frequency of PRDX1-6 in various cancers TCGA data sets that are publicly available in the cBIOPortal (www.cbioportal.org) were analyzed

Samples	Fold Change	P value	Rank
Normal breast stroma vs epithelium	*-3.25*	0.004	271
Breast tumor associated stroma vs normal	*2.23*	0.03	2713
Breast tumor associated stroma relapse vs non-relapse	*-1.47*	0.04	1625
Invasive ductal carcinoma vs adjacent stroma > 10mm	*1.62*	0.015	2874

Table 3. Prdx1 Regulation Across Selected Biosets Data was obtained using the BaseSpace Correlation Engine. Fold change of Prdx1 expression was measured from various different protein tissue expression data sets.

2.0 Identifying the role of Peroxiredoxin-1 in cancer associated fibroblast migration

2.1 Introduction

It is well established that fibroblasts within the tumor stroma acquire an activated phenotype, which is similar to the phenomenon observed in wound healing[20, 146]. In breast carcinomas, only about 20% of stromal fibroblasts maintain an un-activated phenotype; approximately 80% of stromal fibroblasts in the tumoral vicinity will gain this activated phenotype[20, 146]. These activated fibroblasts have been termed cancer-associated fibroblasts (CAFs) due to their nature and relationship to the primary tumor[13, 20]. Fibroblast activation is induced by a broad range of stimuli, which are activated upon tissue injury[20]. When epithelial cells endure injury, they release a wide variety of growth factors such as transforming growth factor-β (TGF-β), epidermal growth factor (EGF), platelet derived growth factor (PDGF) and fibroblast growth factor-2 (FGF-2). Additionally, fibroblasts can also become activated by direct cell-cell communication in addition to direct activation by reactive oxygen species or ECM alterations[20]. Activated fibroblasts are commonly referred to as myofibroblasts due to their expression of α-smooth muscle actin (αSMA). Activated fibroblasts also secrete growth factors such as hepatocyte growth factor (HGF), insulin-like growth factor (IGF), nerve growth factor (NGF), EGF and FGF-2. This increase in growth factor secretion can prompt the activation of proliferation in neighboring epithelial cells[20]. These growth factor secretion cascades observed in activated fibroblasts are of key importance in wound healing responses. In the context of wound healing, fibroblast activation is reversed back to the basal state once the activating stimulus from injury subsides[20]. In cancer, tumors are described as wounds, which do not heal because there is no observed reversion of

activation even when the initial activating stimulus is attenuated and at the molecular level, there is not yet a clear understanding of why and how this occurs[13, 20, 27, 147]. Fibroblasts in a sustained state of perpetual activation continue to secrete and deposit ECM proteins and growth factors resulting in an autocrine-loop stimulating the activation of nearby fibroblasts and preventing the conclusion of the initial injury stimulus[13, 20, 147]. The mechanism by which normal fibroblasts make the conversion to a CAF or their role in the initiation of cancer is still not well understood. However, initial studies have demonstrated that CAFs have the ability to affect the motility of cancer cells via secretion of growth factors into the ECM[148]. Additionally, increased deposition of proteins intrinsic to the ECM, such as collagen and fibronectin, and tumor stromal expansion is often a characteristic of invasive carcinomas[7]. This increase in ECM deposition in tumors is termed desmoplasia; this is often observed in organ fibrosis[14, 149]. Fibrosis and desmoplasia are characterized by thickening and linearization of crosslinked collagen fibers.

A critical step in the initiation of metastasis is the interaction between cancer and stromal cells at the borders of invasion of a perpetually expanding neoplasia. It has been described previously that the aggressiveness of a particular carcinoma is greatly dependent on the ability of malignant cells to recruit surrounding stromal cells and thereby transform them into CAFs[22, 150-152]. During cancer progression, tumor cells modify the surrounding ECM and stroma via secretion of a variety of growth factors and paracrine signaling cascades, which results in the alteration of the microenvironment to a climate which is more favorable and conducive to the metastatic programming of the carcinoma[153]. The role of CAFs promoting collective tumor cell invasion has been previously established[22, 150-152, 154]. A recent study showed that CAFs promote directional cancer cell migration by reorganizing and aligning fibronectin in the ECM[21].

To build upon this theory of CAF induced tumor cell migration, we further examined ROS-induced stromal fibroblast conversion into CAFs and we investigated Prdx1-mediated prevention of tumor initiation and progression. Previous studies conducted by our lab showed that mice lacking Prdx1 had shorted lifespans due to severe hemolytic anemia and the development of several cancers, including breast cancer[106, 155-157]. Currently the relationship between reactive oxygen species (ROS) and CAF development is not well described. Therefore, we found it imperative to better understand the mechanism by which Prdx1 and its mediation of ROS, influences CAF migration. We hypothesized that stromal Prdx1 is inactivated by a cancer-cell secreted factor, thereby, transforming normal fibroblasts to an activated, CAF-like fibroblast, rending these activated fibroblasts more migratory.

2.2 Materials and Methods

2.2.1 Fibroblast Isolation and Cell Culture Conditions

Primary SAFs were isolated from female BALB/c mouse mammary glands. Female BALB/c mice were purchased from Jackson laboratory. Animals were housed in a pathogen-free facility in accordance with the Animal Care and Use Guidelines of the University of Pittsburgh. Mammary stromal fibroblasts were isolated from 8 to 12-week old virgin BALB/c female mice. Briefly, mice were sacrificed, and the mammary glands quickly removed, washed twice in wash solution (46 mL Dulbecco's phosphate buffered saline (DPBS) (Sigma), 2.5mL FBS (Gibco), 100 units/ml penicillin, 100 mg/ml streptomycin (Mediatech) and 400 µL Fungizone), and finely minced. Tissues were then disaggregated by repeated aspiration using a 10 ml syringe (no needle).

Tissues were then centrifuged and digested at 37 °C for 2 h in DMEM containing 10% FBS, 100 units/ml penicillin, 100 mg/ml streptomycin (Mediatech), 3500 units/ml collagenase followed by a 10 min trypsin digestion step that was neutralized with FBS. Cells were then washed twice in PBS and plated in complete DMEM with 5% FBS. After 2 h, non-adherent cells were removed and the remaining fibroblasts were cultured for several weeks at 37 °C in a 5% CO_2 and 5% oxygen until spontaneously immortalized.

2.2.2 Lentivirus Preparation and Infection

Lentivirus of pLKO.1 shRNA vector specific to Prdx1 was prepared in 293T HEK cells in OPTI-MEM Reduced Serum Media. The shRNA Prdx1 target sequence used was, 5'CCGGGCTCAGGATTATGGAGTCCTACTCGAGTAAGACTCCATAATCCTGAGCTTTTTG-3'. Following 24 h, the media was exchanged to 10% FBS-DMEM media and virus was collected at 24 and 48 h. Parental SAFs were then infected with 8 μg/mL polybrene in the media. Following initial infection, medium was exchanged and 7 days post-infection cells were placed under puromycin selection (2 μg/mL) in 10% FBS-DMEM media.

2.2.3 Immunoblot

SAFs were lysed in a TRIS lysis buffer (50mM Tris; 2% Triton X-100; 0.5 mM EDTA; 0.5 mM EGTA; 150 mM NaCl; 10% glycerol; 50 mM NaF; 1 mM NaVO4; 40 mM β-glycerophosphate), supplemented with 30 μg/mL catalase from bovine liver (Sigma), and proteinase inhibitors. Protein concentrations were quantified using the Pierce BCA Protein Assay kit, according to the manufacturer's instructions (ThermoFisher). Whole cell lysates were

fractionated by SDS-PAGE and transferred to a nitrocellulose membrane according to the manufacturer (BioRad). Membranes were blocked with 5% BSA in TBS for 2 h, and incubated with antibodies against Prdx1(1:1000)(Abcam), PRDX-SO3 (1:1000)(Abcam), and GAPDH (1:1000)(Abcam), overnight at 4 °C. Membranes were washed three times for 10 min in TBST (0.05% Tween-20), and visualized by infrared (IR) detection. For IR processing, membranes were incubated with a 1:15000 dilution of anti-goat, anti-rabbit, or anti-mouse IRDye (LI-COR), for 30 min at 25˚ C. Blots were washed with TBST 3-times and with TBS once, and imaged on an Odyssey (LI-COR) imager.

2.2.4 Immunofluorescence

SAFs were seeded on glass cover slips and were fixed for 15 minutes in 3.7% paraformaldehyde, rinsed twice in cold PBS pH=7.4 for 10 min and permeabilized in blocking solution (PBS with 5% BSA and 0.3% Triton™ X-100) for 30 min. Cover slips were then washed twice in chilled PBS pH=7.4 for 10 min and specific primary antibodies (anti-collagen-1 (Calbiochem), α-smooth muscle actin - Cy5 (Sigma-Aldrich), vimentin (Cell Signaling) were diluted 1:250 in antibody dilution buffer: (PBS with 5% BSA and 0.3% Triton™ X-100) were applied overnight at 4°C. Cells were washed twice in cold PBS pH=7.4 for 10 min and flourochrome-conjugated secondary antibodies (mouse or rabbit) Alexa Fluor® (Molecular Probes, Life Technologies) diluted 1:2000 in antibody dilution buffer were applied for 2 h at RT in the dark. To visualize DNA, after two 10 min washes, cells were stained with Hoechst (Molecular Probes, Life Technologies) for 15 min at RT in the dark. The slides were again rinsed in PBS and then the cover slips were mounted on microscope slides using Prolong® Gold Anti-

Fade Reagent (Molecular Probes, Life Technologies). Images were obtained on an Olympus confocal microscope.

2.2.5 Luminol Hypochlorite Assay

Hydrogen peroxide was measured using a GloMax (Promega) with injectors from 200,000 MFFs in a 12-well plate in 1 ml of serum-free DMEM utilizing a modified luminol/hypochlorite assay. Briefly, DMEM diluted with PBS to 25% was added to a 96-well plate and luminescence was measured by injecting luminol (Sigma) and sodium hypochlorite (Sigma) to final concentrations of 120 μM and 250 μM, respectively. Hydrogen peroxide concentrations were determined by comparison to experimental standard curves (0 to 100 μM).

2.2.6 Transwell Migration Assay

SAFs were starved in 0.25% FBS DMEM for 24 h at 37°C, 21% CO_2. Cells were trypsinized, spun for 5 min at 1500xg and suspended in 0.25% FBS DMEM. Cells were counted and 2.5 x 10^4 fibroblasts in 0.25% FBS DMEM were seeded onto the membrane of the self-standing Millicell Culture Plate Inserts (Millipore). 2 ml of 10% FBS DMEM was added to the bottom of the plate. The migration assay was carried out for 24 h at 37°C, 21% CO_2. Following the 24 h migration, a damp cotton swab was used to wipe the non-migrated cells from the top of the transwell membrane. Cells were fixed with 2% paraformaldehyde for 15 min, washed twice with 1X PBS, and stained with 0.1% crystal violet. Numbers of migrating SAFs were visualized under a light microscope using 4X magnification. Images of the crystal violet stained membrane were quantified using ImageJ to assess number of migrating SAFs.

2.2.7 Statistical Analysis

Student's t-test was used to compare two groups. Data are presented as mean +/- SD. Statistical analyses were done using GraphPad Prism. p-value < 0.05 was considered significant

2.3 Results

2.3.1 Loss of Prdx1 in SAFs leads to increased migration

Prdxs are a family of peroxidases ranging between 22-27 kDa and there are six known mammalian isoforms[17, 18, 20]. Although the individual roles among the isoforms are quite distinct, overall, they all catalyze the reduction of H_2O_2 to H_2O via their peroxide function and they are all found to be ubiquitously expressed throughout the cell[17-20]. All aerobic organisms produce H_2O_2, as a byproduct of normal cellular metabolism. Due to its cellular toxicity, these organisms are equipped with detoxifying enzymes such as catalase, glutathione peroxidases and peroxiredoxins; these enzymes function to metabolize H_2O_2, thereby ameliorating cellular toxicity[21]. Although H_2O_2 is toxic to cells, it can provide a critical function as a signaling molecule via oxidation of critical cysteine residues of protein tyrosine phosphatases in response to cell surface receptor activation[21].

In the context of Prdx1, the active site cysteine is selectively oxidized to cysteine sulfinic acid rendering the peroxiredoxin inactive and unable to scavenge H_2O_2[22]. Oxidative stress in CAFs is known to drive tumor progression due to its influence on the stromal microenvironment and through the induction of genomic instability in neighboring cancer cells thereby elevating their

aggressive behavior; CAFs are much more genomically stable in comparison to epithelial cancer cells[23]. In breast cancer, loss of Cav-1 is one of the strongest stromal biomarkers associated with poor clinical prognosis.

Cancer cells have been shown to induce ROS production in stromal fibroblasts, ultimately leading to a decrease in stromal Cav-1 expression[23]. Cancer cells have been shown to adopt compensatory mechanisms against excessive oxidative stress leading to cellular damage by upregulating antioxidant enzymes such as Prdx1[23]. Previous studies from our group have described that the loss of Prdx1 in mice resulted in shortened lifespans due to the development of hemolytic anemia and variety of cancers including breast cancer[17]. Loss of H_2O_2 scavenging capabilities in stromal fibroblasts has yet to be fully understood and as a result, the data presented in this section will explore the phenotypic function that results from Prdx1 loss in stromal fibroblasts. We hypothesized that loss of Prdx1 in stromal fibroblasts would cause them to be more migratory and CAF-like (Figure 4).

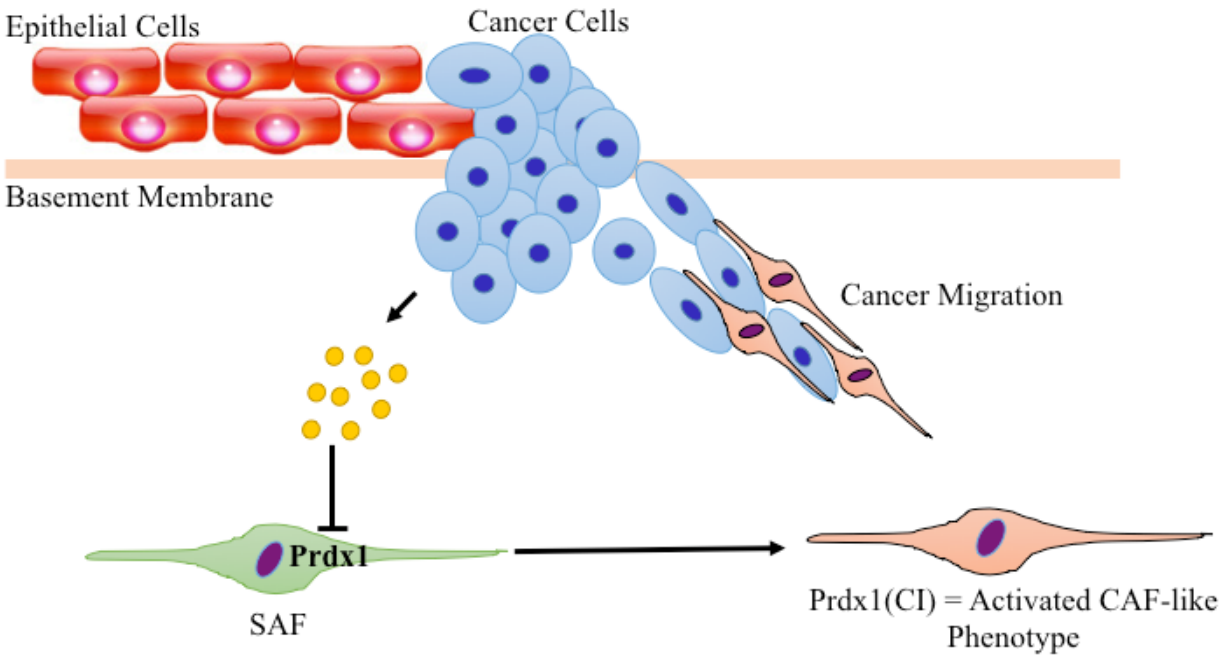

Figure 4. Schematic Illustrating Loss of Prdx1 Stroma-Associated Fibroblasts (SAFs) are transformed into a CAF-like phenotype via the inactivation of Prdx1 in stromal fibroblasts, this is hypothesized to occur via a cancer-cell secreted factor. CI= catalytic inactivation

2.3.2 Prdx1 is inactivated by hydrogen peroxide

As discussed earlier, Prdx1 functions as a H_2O_2 scavenger. The peroxidase activity of Prdx1 can be irreversibly inactivated via exposure to high concentrations of H_2O_2. In Figure 5B, we show that with a 30 min, 100 μM dose of H_2O_2, there is overoxidation of Prdx1 to its Prdx1-SO_3 sulfonic form. At low concentrations of H_2O_2, stromal fibroblasts are able to continue with peroxide scavenging capabilities and the catalytic cysteine does not become overoxidized. However, with high concentrations of H_2O_2, a clear pattern emerges, control EV SAFs become

overoxidized on the catalytic residue of Prdx1 and begin to resemble shPrdx1 SAFs and are no longer able to scavenge and metabolize H_2O_2 (Figure 5A).

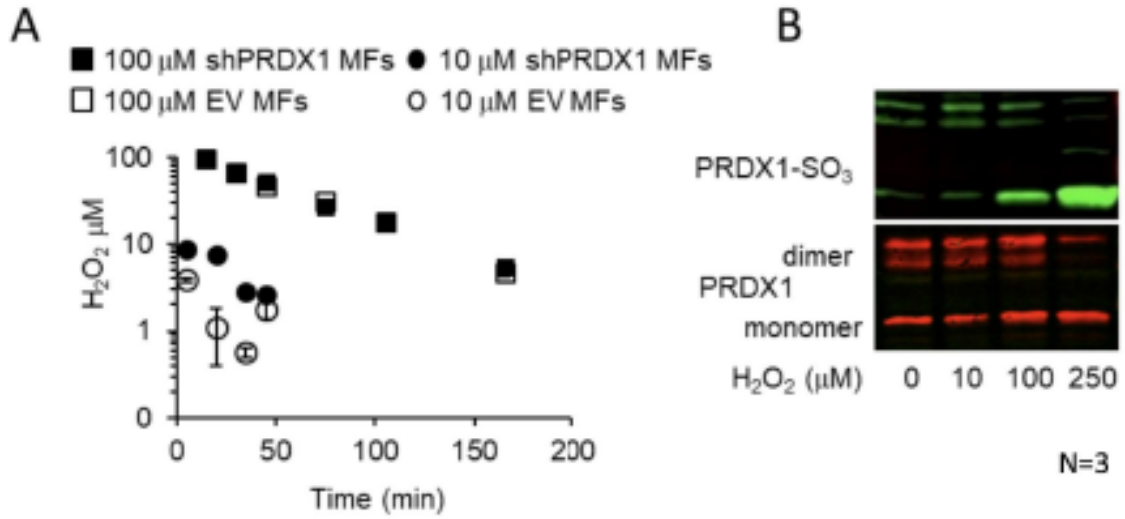

Figure 5. High concentrations of H_2O_2 cause overoxidation of Prdx1 A) At 30 min, 100 μM H_2O_2 treatment, scavenging ability of control SAFs resemble shPrdx1 SAFs B) 30 min treatment of BALB/c stromal fibroblasts with 100 and 250 μM H_2O_2 causes overoxidation of the catalytic cysteine in Prdx1 rending it catalytically inactive and unable to scavenge excess H_2O_2. N=3

2.3.3 Short hairpin knockdown of Prdx1 results in CAF-like phenotype

Short hairpin RNA knockdown of Prdx1 was induced in SAFs via lentiviral infection. Loss of Prdx1 in SAFs resulted in an altered, more CAF-like phenotype. shPrdx1 SAFs were visually more elongated with increased number of spindle-like protrusions (Figure 6A). Immunofluorescence microscopy was conducted to visualize the CAF marker, α-smooth muscle actin (α-SMA). In Figure 6B, it is clear shPrdx1 SAFs express more α-SMA than do the EV

controls. Immunoblot analysis verified the reduction of Prdx1 protein expression in shPrdx1 SAFs (Figure 6C).

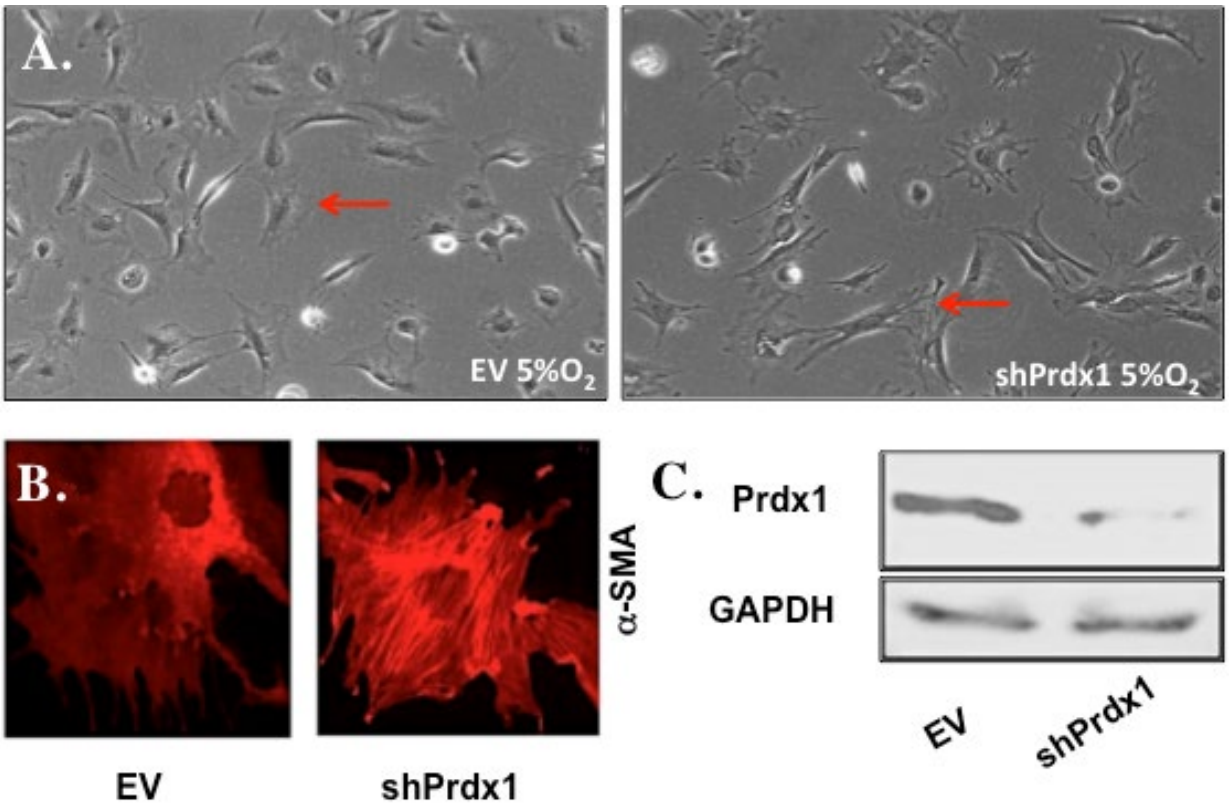

Figure 6. Loss of Prdx1 protein expression results in CAF-like phenotype in stromal fibroblasts A) Phase-contrast microscopy images displaying altered SAF phenotype, shPrdx1 stromal fibroblasts appear more CAF-like with more elongated fibroblasts with enhanced protrusions (arrows) compared to EV-control. B) Immunofluorescence microscopy for α-SMA expression, shPrdx1 leads to increased α-SMA protein expression compared to EV-control. C) Immunoblot confirming reduction of Prdx1 protein expression in shPrdx1 SAFs. N=3

2.3.4 Knockdown of Prdx1 in SAFs leads to increased migration

Loss of Prdx1 in both human and murine SAFs resulted in significantly increased migration in transwell assays. In the human SAFs, VI-RMF, there was approximately a two-fold increase in transwell migration compared to the EV-control (Figure 7A). A similar migratory phenotype was observed in the shPrdx1 BALB/c mouse SAFs; loss of Prdx1 resulted in significantly more migration compared to EV-control SAFs. Treatment with increasing doses of H_2O_2 resulted in a significant, sustained elevation of migration in shPrdx1 SAFs. Although not statistically significant, with increasing doses of H_2O_2, the EV-control SAFs trended towards increased migration (Figure 7B). The bottoms of the transwell membranes were stained with crystal violet and migrated cells were visualized as those stained purple. shPrdx1 BALB/c mouse SAFs migrated significantly more than the control EV SAFs (Figure 7C).

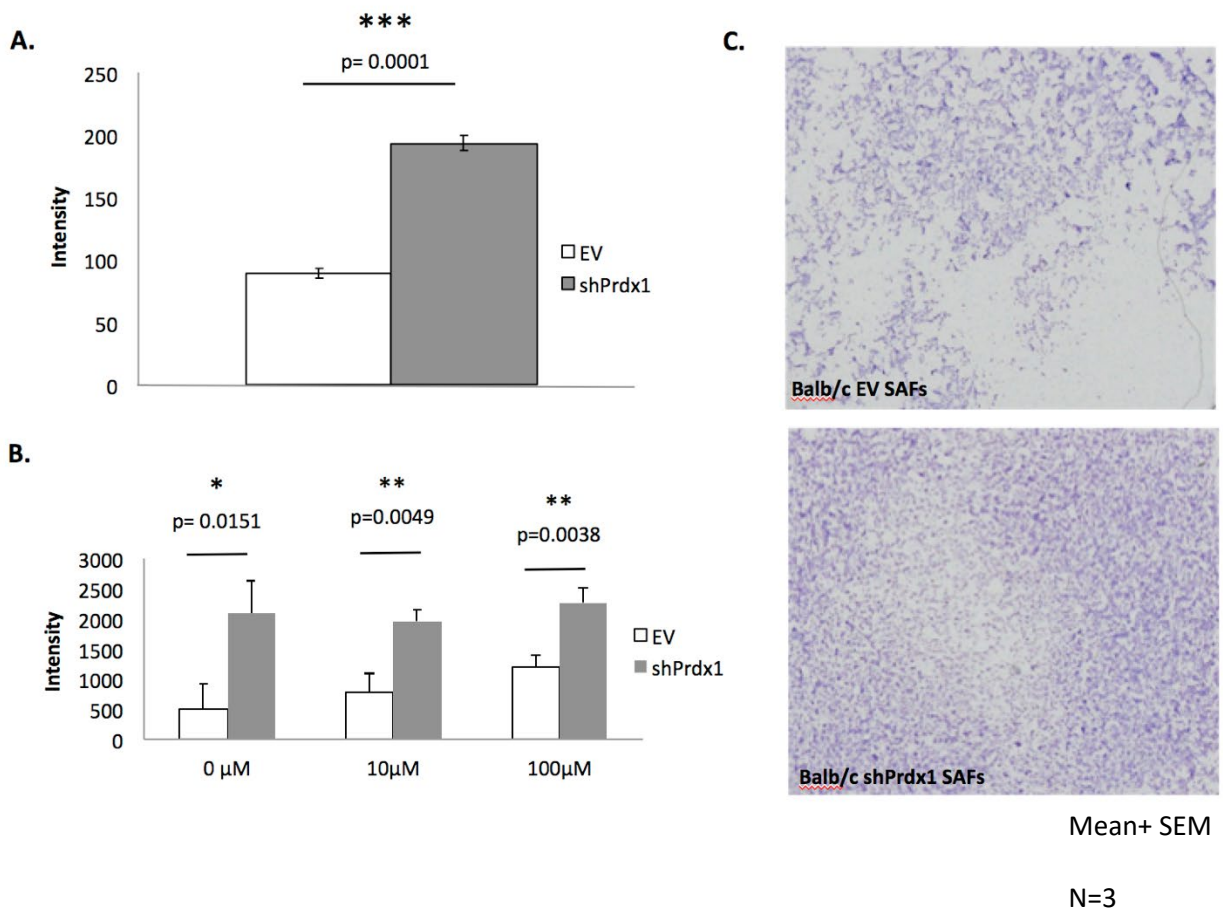

Figure 7. Loss of Prdx1 leads to significantly increased migration in human and murine SAFs A) shPrdx1 VI-RMF Human SAFs were significantly more migratory than EV-control SAFs. B) shPrdx1 BALB/c mouse SAFs were significantly more migratory than EV-control SAFs. Treatment with increasing doses of H2O2 sustained a significant increase in migration compared to the EV SAFs. C) Crystal violet staining of transwell membrane for visualization of migrated cells BALB/c SAFs.

2.4 Discussion

The tumor microenvironment is comprised of both cellular and non-cellular components, for example, fibroblasts and collagen, respectively[13, 21, 151, 156]. The architecture of the ECM has been shown to have a significant influence on critical cellular functions such as proliferation,

migration, differentiation and cancer progression[13, 20, 21, 147, 158]. Aberrant ECM remodeling is a hallmark of aggressive cancers[13, 20, 81, 158-160]. CAFs play an important role in this remodeling, mostly because of their ability to deposit matrix proteins such as collagen and fibronectin[13]. The significant influence of the stroma on the development and progression of a wide range of various cancer types has been well supported by a large body of clinical evidence showing that in tissues with chronically inflamed stroma, there is a higher incidence of tumor development[161-163].

Histologically, there are striking similarities between the tumor stroma and wound healing stroma; both of these environments contain a large population of myofibroblasts[9]. Myofibroblasts are of particular interest in the reactive stroma of cancer because these cells are typically found at sites of tissue remodeling. In wound healing, myofibroblasts are generated from granulation of tissue fibroblasts and in the context of cancer, carcinoma cells have been shown to induce the transformation of normal fibroblasts to reactive myofibroblasts[16, 23, 164, 165].

Myofibroblasts are known to synthesize and secrete components of the ECM such as collagen-I, collagen-III, tenascin and versican while also regulating the expression of proteases[15, 16, 37, 51, 52, 81]. Production of these matrix components can result in the remodeling of the ECM, which can promote cancer cell proliferation, growth, migration and invasion,[16, 51, 53, 54, 56, 81, 166]. The aberrant remodeling that occurs in cancer further supports the critical role myofibroblasts play in promoting an environment conducive to tumor progression[16]. Studies with co-cultures of carcinoma and stromal cells revealed that tumor cell migration is always primarily led by a fibroblast and that the carcinoma cells migrate within tracks within the ECM trailing behind a fibroblast[150]. Furthermore, the tracks and remodeled collagen generated by the leading fibroblasts provide a migratory structure allowing the collective invasion of carcinoma cells, thereby promoting tumor progression.

The data presented in this chapter describes a similar migratory phenotype, which occurs upon loss of Prdx1 in stromal fibroblasts. A significant increase in migration is observed in transwell assays in using both human and mouse stromal fibroblasts deficient in Prdx1. This migratory phenotype strongly suggests that Prdx1 can function to prevent cancer progression by regulation of fibroblast-led migration. In addition to increased migration, loss of Prdx1 also results in phenotypic changes, such as elongation and the formation of migratory protrusions, due to cytoskeletal remodeling. These phenotypic differences can be appreciated when compared to control fibroblasts (Figure 6). Overall, these data define the critical role of Prdx1 in cancer cell migration and in tumor progression. Loss of stromal Prdx1 provides a stromal environment permissive to cancer progression, allowing ECM matrix remodeling and cancer cell migration to occur. In the following chapters we will deeply investigate and characterize the phenotypes and mechanisms of Prdx1 mediated breast cancer cell progression and present novel data which further support the importance and influence of the ECM on tumor progression and the critical role of Prdx1 in preventing metastasis.

3.0 Cancer cell conditioned media inactivation of Prdx-1

3.1 Introduction

All six Prdx family members share a conserved catalytic cysteine residue on the N-terminal region termed the peroxidatic cysteine, Cys52[128]. Prdxs 1-4 contain an additional conserved cysteine residue on the C- terminal region which is termed the resolving cysteine, Cys 173[128]. With increasing doses of H_2O_2, Prdxs can become easily over oxidized on the catalytically active cysteine from a sulfhydryl to sulfinic to a sulfonic acid[167, 168]. This observed overoxidation is thought to be due to the existence of a thiolate anion on Cys51, while the other cysteine residues, Cys71, Cys83 and Cys 173, remain in a protonated state at neutral pH. The catalytic Cys52 is extremely reactive with H_2O_2 to undergo a complete overoxidation to sulfonic acid or to form a disulfide bond[169]. Cellular levels of H_2O_2 are tightly regulated by peroxidases; Prdxs scavenge low concentrations of H_2O_2 whereas catalase scavenges high concentrations of H_2O_2[119, 128]. Reversible inactivation through overoxidation appears to be an adaptation in eukaryotic cells to allow the substantial accumulation of H_2O_2, thereby allowing H_2O_2-dependent signaling to occur[138]. Inactivation of Prdx1 by H_2O_2 induced overoxidation has been well described in the literature[119, 167, 170]. Growth factor induced phosphorylation and inactivation of Prdx1 on Y194 has only been described in the context of wound healing by one study published in 2010[138]. Because of the importance of Prdx1 in the context of cancer cell signaling and migration, in the results presented

in this section, we investigate the influence of MB-MDA-231 breast cancer cell conditioned media on Prdx1 status in SAFs at the tumor-stroma interface. Here we hypothesize a novel mechanism by which Prdx1 can become inactivated via a paracrine loop from cancer-cell secreted factors, thereby mediating Prdx1-dependent collagen remodeling.

3.2 Materials and methods

3.2.1 Cell Culture Conditions

Primary SAFs were isolated from female BALB/c mouse mammary glands as previously described in Chapter 2. SAFs were cultured at 37 °C in a 5% CO_2 and 5% oxygen incubator.

3.2.2 Lentivirus Preparation and Infection

Lentivirus of pLKO.1 shRNA vector specific to Prdx1 was prepared in 293T HEK cells in OPTI-MEM Reduced Serum Media. The shRNA Prdx1 target sequence used was, 5'CCGGGCTCAGGATTATGGAGTCCTACTCGAGTAAGACTCCATAATCCTGAGCTTTTTG-3'. Following 24 h, the media was exchanged to 10% FBS-DMEM media and virus was collected at 24 and 48 h. Parental SAFs were then infected with 8 μg/mL polybrene in the media. Following initial infection, media was exchanged and 7 days post-infection cells were placed under a puromycin selection (2 μg/mL) in 10% FBS-DMEM media.

3.2.3 Immunoblot

SAFs were lysed in a TRIS lysis buffer (50mM Tris; 2% Triton X-100; 0.5 mM EDTA; 0.5 mM EGTA; 150 mM NaCl; 10% glycerol; 50 mM NaF; 1 mM $NaVO_4$; 40 mM β-glycerophosphate), supplemented with 30 μg/mL catalase from bovine liver (Sigma), and proteinase inhibitors. Protein concentrations were quantified using the Pierce BCA Protein Assay kit, according to the manufacturer's instructions (ThermoFisher). Whole cell lysates were separated by SDS-PAGE and transferred to a nitrocellulose membrane according to manufacturer (BioRad). Membranes were blocked with 5% BSA in TBS for 2 h, and incubated with antibodies against phospho-Prdx1-Y194 (1:1000; Cell Signaling), Prdx1 (1:1000; Abcam), Prdx-SO_3 (1:1000; Abcam), and β-Actin (1:1000; Abcam), pSrc (Cell Signaling; 1:1000), Src (Cell Signaling; 1:1000) overnight at 4 °C with rocking. Membranes were washed three times for 10 min in TBST (0.05% Tween-20), and visualized by IR detection. For IR processing, membranes were incubated with a 1:15000 dilution of anti-goat, anti-rabbit, or anti-mouse IRDye (LI-COR), for 30 min at 25˚ C. Blots were washed with TBST 3 times and with TBS once, and imaged on an Odyssey (LI-COR) imager. Membranes processed by chemiluminescence were incubated in a 1:1000 dilution of HRP-conjugated TrueBlot (Rockland) anti-mouse or anti-rabbit antibodies for 1 h at 25˚ C. Blots were washed three times with TBST for 5 min, and exposed to ECL for 1 min.

3.2.4 Statistical Analysis

Student's t-test was used to compare two groups. Data are presented as mean +/- SEM. Statistical analyses were done using GraphPad Prism. p-value < 0.05 was considered significant. Data reported are representative images of at least 3 biologic replicates, $n \geq 3$.

3.3 Results

3.3.1 Prdx1 inactivation occurs at tumor-stroma interface

Prdx1 is hypothesized to become inactivated at the tumor-stroma interface via cancer-cell secreted factors. We initially thought that Prdx1 was inactivated via a H_2O_2-dependent mechanism of overoxidation to Prdx-SO_3. Data will be presented in this section revealing a novel mechanism of Prdx1 inactivation in the context of breast cancer (Figure 8).

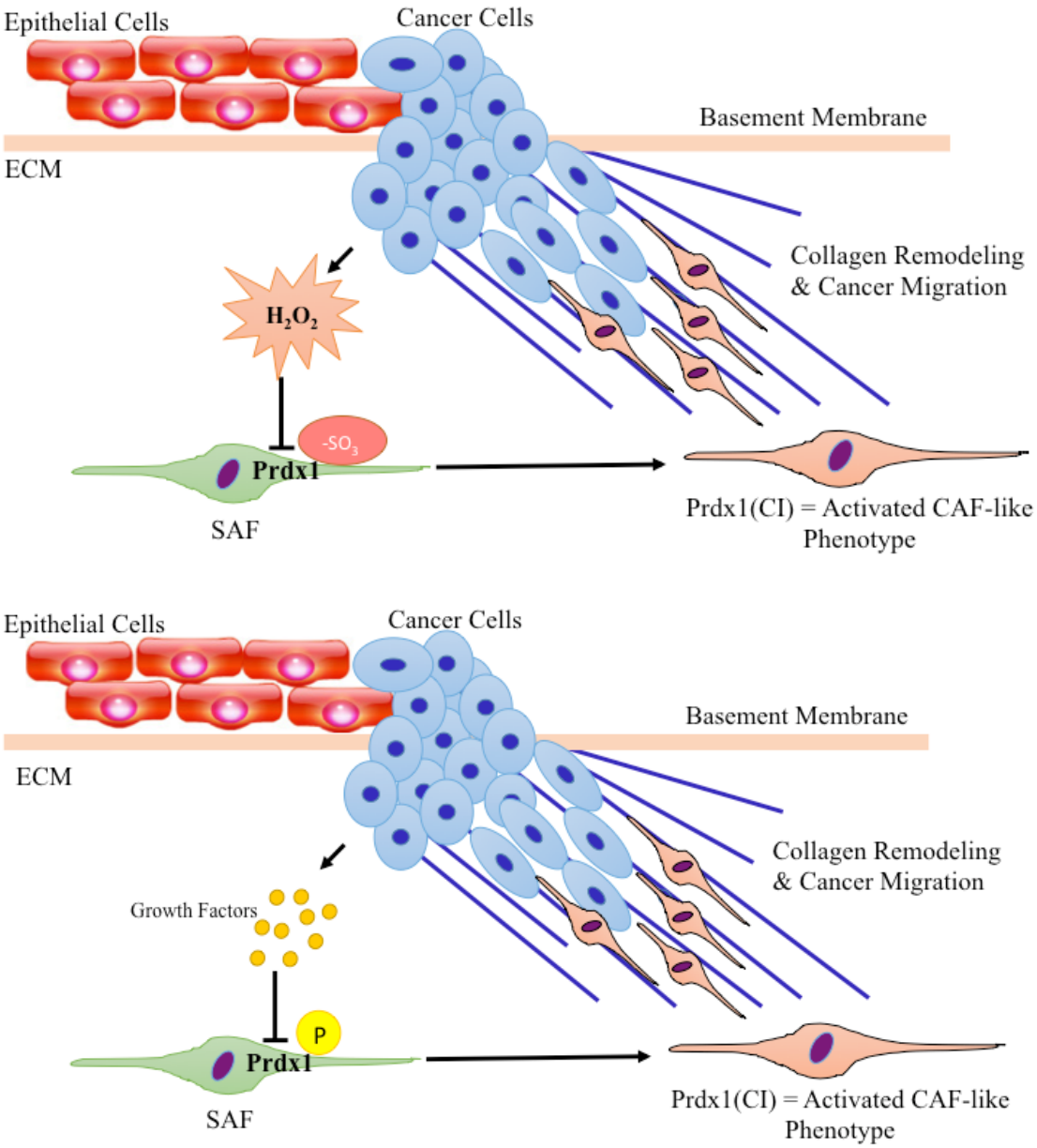

Figure 8. Schematic of hypothesized mechanism of Prdx1 inactivation Under basal conditions, stromal Prdx1 activity is high. In progressive metastatic disease and cancer load, stromal Prdx1 activity is low leading to increased ECM and collagen remodeling. There are two possible mechanisms of Prdx1; (Top) Cancer-cell secreted H2O2 inactivates Prdx1 to Prdx-SO3. (Bottom) Cancer-cell secreted growth factor inactivates Prdx1 via phosphorylation on Y194.

3.3.2 Prdx1 is not inactivated via MBA-MD-231 conditioned media in a H_2O_2-dependent manner

As described previously, Prdx1 can become inactivated by a H_2O_2-dependent mechanism or by phosphorylation on Y194[119, 138, 167, 170]. Based on literature suggesting that ROS are an important contributor to CAF evolution, we initially hypothesized that breast cancer cells secrete H_2O_2, which inactivates Prdx1 in fibroblasts and causes fibroblast migration and cancer cell metastasis. To test this, we examined Prdx1 overoxidation upon treatment with MB-MDA-231 breast cancer cell conditioned media. The results were striking; inactivation of Prdx1 did not occur via H_2O_2 –dependent overoxidation (Figure 9).

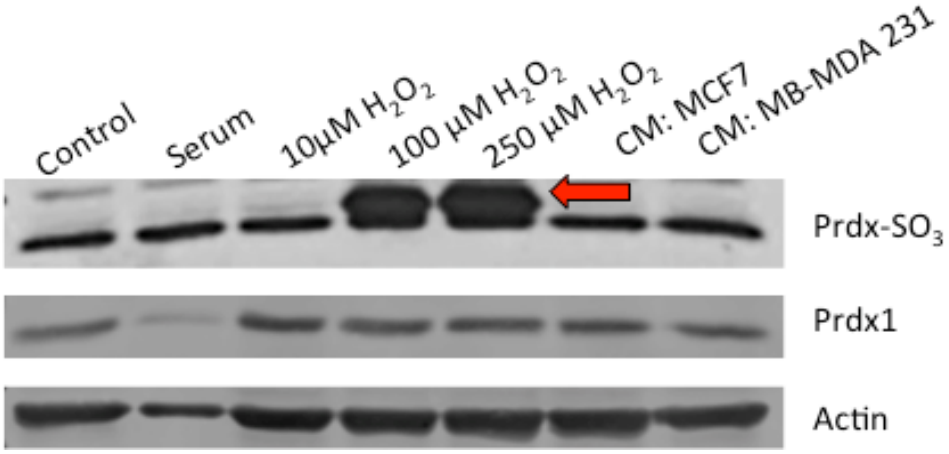

Figure 9. Prdx1 inactivation does not occur via overoxidation by H_2O_2 Treatment with cancer conditioned media (MCF-7 & MDA-MB-231) does not cause overoxidation (Prdx-SO_3). Positive controls for oxidation are 100 and 250 μM H_2O_2. N=6

3.3.3 Prdx1 is inactivated via phosphorylation on Y194 by MDA-MB-231 cancer cell secreted factors.

Prdx1 can become inactivated via phosphorylation on Y194 as was described previously in the context of wound healing[138]. Here, we have shown that phosphorylation of Prdx1 occurs in the context of breast cancer. Using both non-aggressive and aggressive breast cancer cell lines, MCF-7 and MDA-MB-231, respectively, we show that phosphorylation of Y194 in parental SAFs occurs upon treatment with MDA-MB-231 conditioned media and not with MCF-7 conditioned media. (Figure 10A,B). Moreover, we show that treatment with MDA-MB-231 conditioned media resulted in significantly higher phosphorylation of Y194 in parental SAFs compared to the control treated samples (10A,B). Src phosphorylation was also significantly higher in MDA-MB-231 conditioned media treated SAFs (10 C,D).

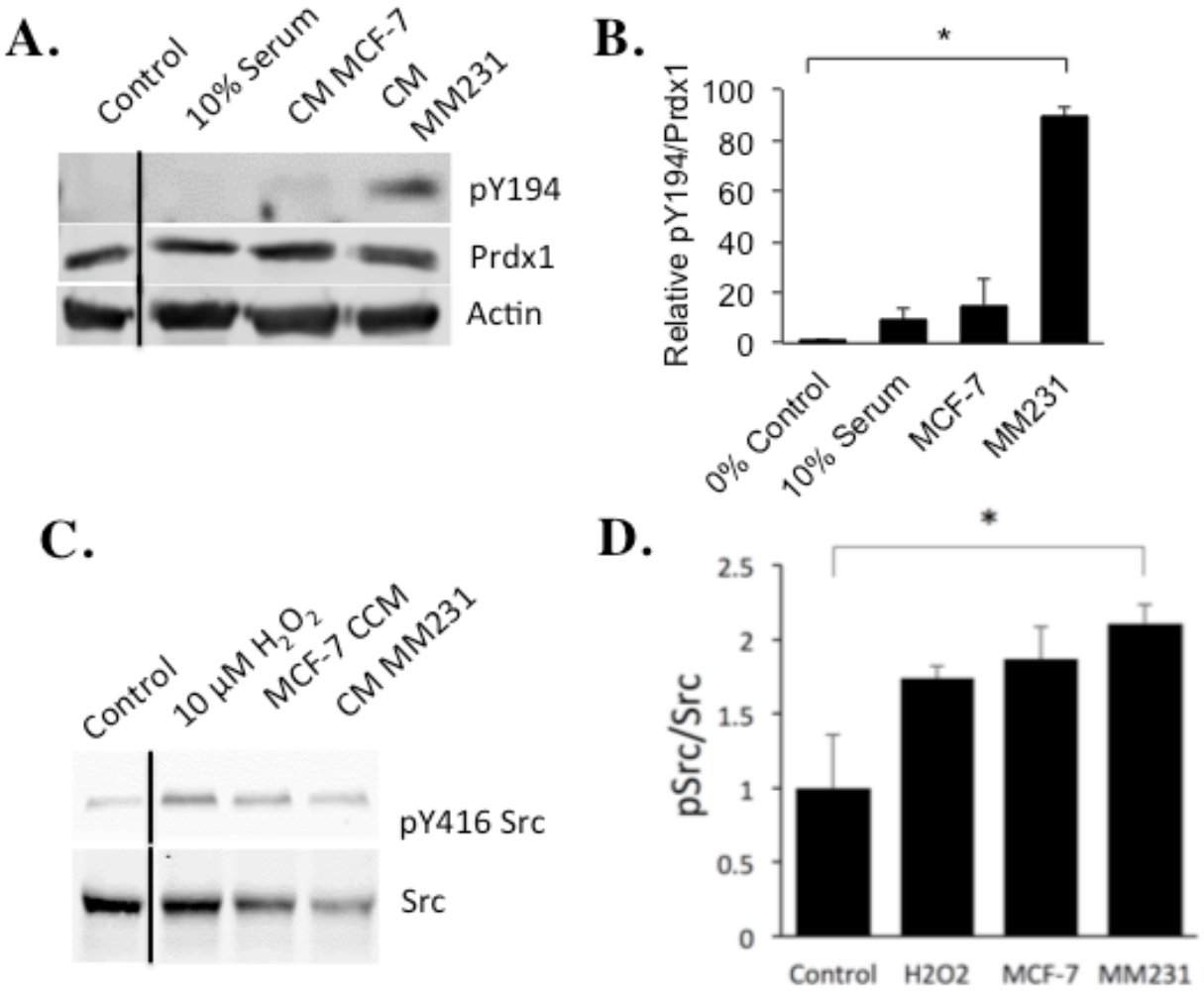

Figure 10. Prdx1 is inactivated via cancer cell secreted factors by phosphorylation of Y194. A). Prdx1 inactivation via phosphorylation on Y194 occurs upon treatment with MDA-MB-231 cancer conditioned media and not with MCF-7 cancer conditioned. B) Quantification of western blot, MDA-MB-231 conditioned media treatment resulted in significantly higher phosphorylation of Y194 compared to control and serum treated SAFs. C) Src phosphorylation was also significantly higher in MDA-MB-231 conditioned media treated SAFs. D) Quantification of Src-phosphorylation western blot indicating significantly higher pSrc/Src in MDA-MB-231 conditioned media treated SAFs compared to control.

3.3.4 Prdx1 is inactivated via Src-dependent phosphorylation of Y194

To further understand the mechanism by which Prdx1-Y194 phosphorylation occurs, we pretreated SAFs and MDA-MB-231 conditioned media with 20 μM PP1 and detected by immunoblot. PP1 is a Src selective kinase inhibitor which has been used to investigate signaling pathways involving Src kinases[171]. Upon treatment with 20 μM PP1, there is a significant reduction in phosphorylation on Y194 of Prdx1 (Figure 11). Moreover, further supporting our hypothesis that pY194-Prdx1 is Src dependent, there is also a significant reduction in pSrc (Figure 11). Our data thus far shows that the inactivation of Prdx1 is in fact due to breast cancer cell secreted factors, either due to a growth factor or H_2O_2. Overall, we confirm that Src regulates the phosphorylation of Prdx1 as shown by our inhibition studies and that phosphorylation is indeed due to paracrine signaling from a cancer-cell secreted factor.

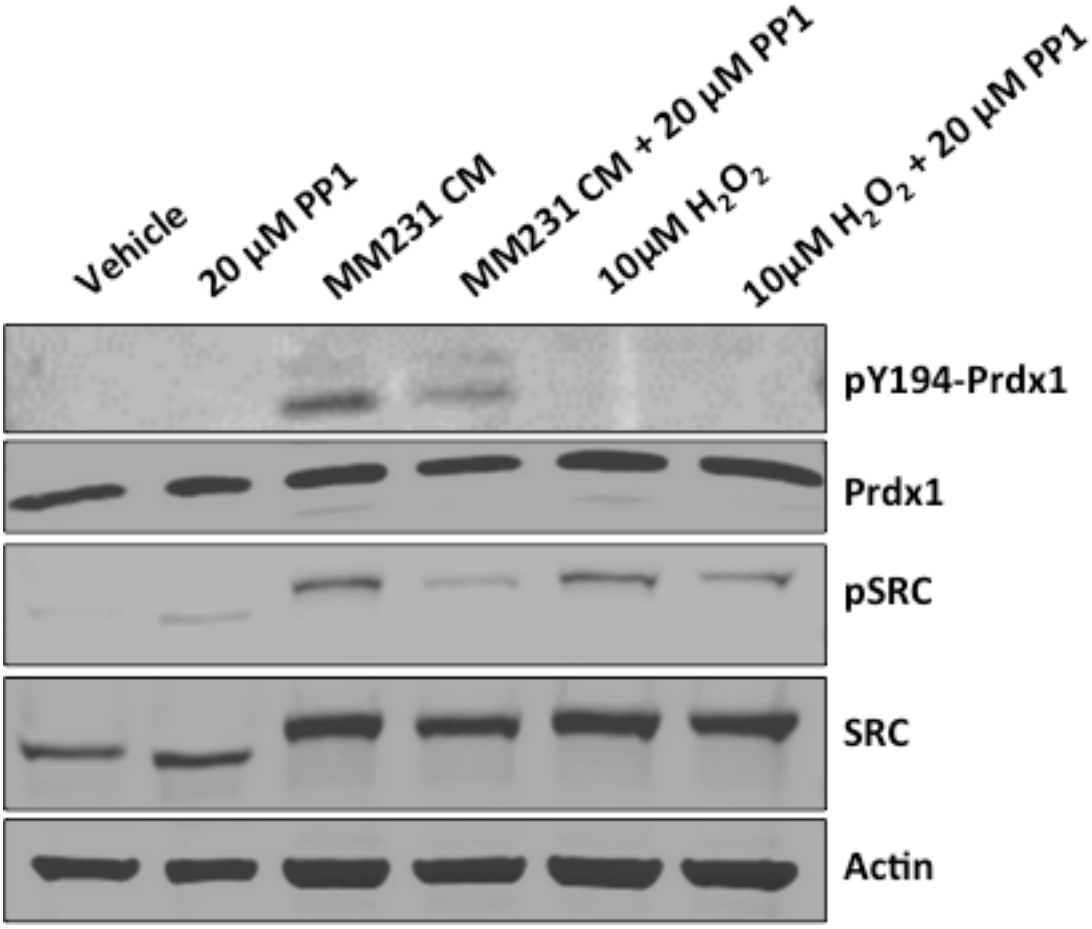

N=4

Figure 11. Y194 phosphorylation of Prdx1 is Src- dependent A) Parental SAFs were seeded at a density of $5x10^5$ cells per plate and were pre-treated for 2 h with 20 µM PP1 and subsequently treated with MDA-MB-231 conditioned media for 30 mins. Treatment with PP1 resulted in a significant reduction in both pY194-Prdx1 and also in pSrc.

3.3.5 Three potential pathways for inactivation of Prdx1

In the data presented, we have explored three potential pathways for Prdx1 inactivation. The first and most commonly described in the literature is the H_2O_2–dependent overoxidation of Prdx1, which converts Prdx1 to its sulfonic form ($-SO_3$), inactivating peroxidase activity of Prdx1. We initially explored this pathway by treating parental SAFs with MDA-MB-231 conditioned media and detecting by immunoblot for Prdx-SO_3 (Figure 6). The results clearly showed that Prdx1 inactivation via H_2O_2 to overoxidation of Prdx was not the mechanism responsible for Prdx1 inactivation at the tumor-stroma interface (Figure 12). Next, we explored if inactivation of Prdx1 was due to phosphorylation on Y194. Treating with conditioned media from both MCF-7 and MDA-MB-231 breast cancer cell lines, we evaluated pY194-Prdx1 by immunoblot and found that Prdx1 was indeed phosphorylated on Y194, however only by MDA-MB-231 conditioned media and not by MCF-7 conditioned media. Moreover, our data suggests that phosphorylation of Prdx1 occurs via a Src-dependent mechanism.

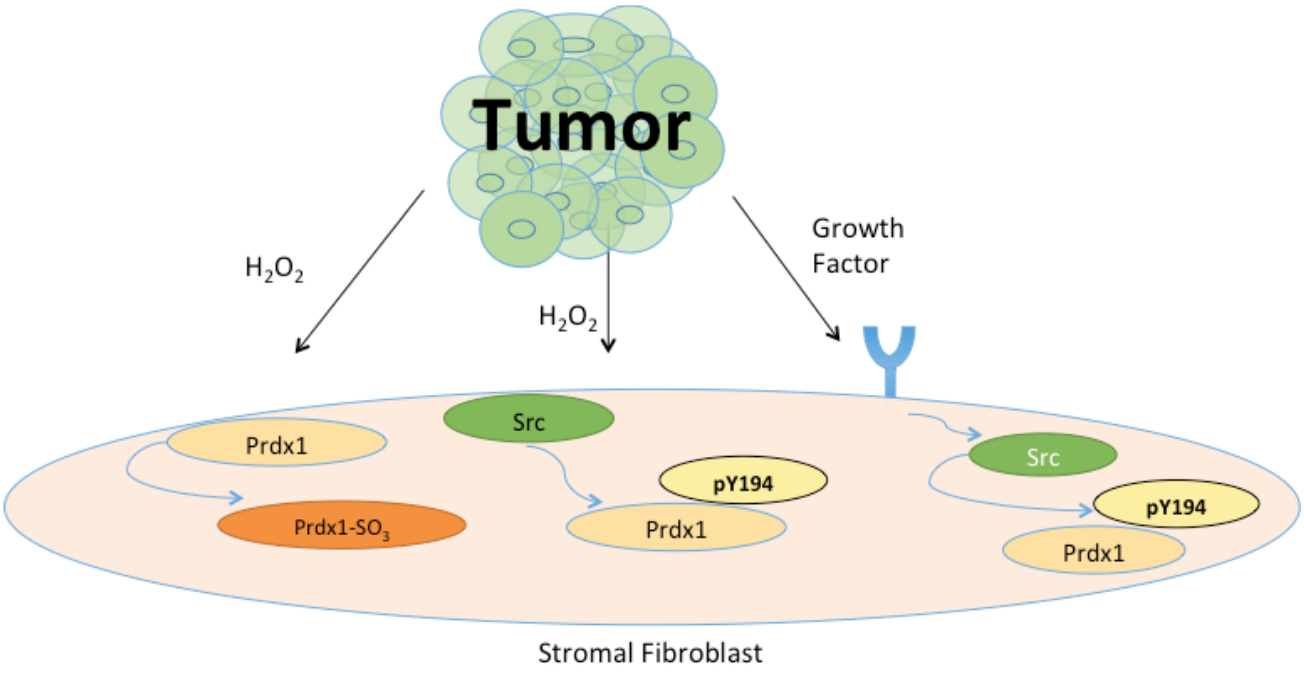

Figure 12. Potential pathways of Prdx1 inactivation Prdx1 can become inactivated by H2O2 causing either overoxidation (Prdx-SO3) or via Src activation leading to Prdx1 inactivation via phosphorylation of Y194. Prdx1 can also become phosphorylated by growth factor activation of Src leading to inactivation of Prdx1 via phosphorylation on Y194.

3.4 Discussion

H_2O_2 is a metabolic byproduct of cellular respiration and has been generally considered toxic to cells; however, evidence has emerged suggesting that the production of such reactive oxygen species (ROS) play a critical role in membrane-receptor signaling[128, 156, 157, 172-174]. Prdx1 is a peroxidase whose main function is to scavenge excess H_2O_2, however, upon exposure to high concentrations of H_2O_2, Prdx1 becomes overoxidized and loses its peroxidatic and scavenging capability[106, 113, 128, 155-157, 175]. This inactivation of Prdx1 allows for the transient accumulation of H_2O_2 in cellular membranes allowing signaling to occur[119, 167, 170, 172].

As discussed in previous chapters, the most widely accepted mode of Prdx1 inactivation is via overoxidation to Prdx1-SO_3. Another route by which Prdx1 can become inactivated is by phosphorylation of Y194; to date, there has only been one study which describes phosphorylation of Prdx1 on Y194 in the context of the wound healing edge[138]. In this chapter, we describe a novel mechanism of Prdx1 inactivation via phosphorylation of Y194 (pY194-Prdx1) in the context of breast cancer.

Our finding is of critical translational importance because of its influence on cancer metastasis and migration. Here we investigated the signaling that takes place at the tumor-stroma interface. Initially, we hypothesized that the highly aggressive breast cancer cell line, MDA-MB-231, would inactivate Prdx1 by H_2O_2-mediated overoxidation of its catalytic cysteine; however, we discovered that this did not occur (Figure 9). On the contrary, as described in Figure 10, Prdx1 became inactivated via phosphorylation of Prdx1on Y194. This finding suggested that Prdx1 either became inactivated by a cancer secreted growth factor, causing the activation of Src and ultimately leading to the phosphorylation of Prdx1 or via H_2O_2-mediated Src activation causing phosphorylation of Prdx1 (Figure 12). In the context of wound healing, Prdx1is transiently

phosphorylated during active wound regeneration and once the wound is healed, phosphorylation of Prdx1 is no longer observed[138]. The data presented in this chapter illustrates a mechanism by which a MBA-MD-231 breast cancer-cell secreted factor inactivates Prdx1, rendering it catalytically inactive, thereby, permitting a host of tumor permissive events to occur, which will be discussed in detail in chapter 4. Because cancer is typically described as a wound, which does not heal, this observation is of particular interest when exploring the signaling dynamics of the tumor and surrounding stromal interface of the ECM.

To delve deeper into understanding how MDA-MB-231 breast cancer cells regulate phosphorylation of Prdx1, we treated SAFs with both the Src inhibitor, PP1 (Figure 11). These results suggested that inactivation of Prdx1 by phosphorylation of Y194 was most likely due to a breast cancer-cell secreted growth factor or H_2O_2 leading to SRC activation and ultimately Prdx1 inactivation via phosphorylation. Two likely candidates, as described in the context of wound healing, are epidermal growth factor (EGF) or platelet derived growth factor (PDGF)[138].

Abnormal accumulation of ROS in tumor epithelial cells, inducing aberrant signaling cascades and leading to oncogenic phenotypes has been well-described[147, 156, 176]. Moreover, ROS can also affect the cellular composition of fibroblasts in the tumor stroma of the ECM by transforming them into CAFs[176]. Based on our finding thus far, we have established that phosphorylation-dependent inactivation of Prdx1 is mediated by an MBA-MD-231 breast cancer cell-secreted factor. H_2O_2, is a known activator of Src, therefore, it is also possible that phosphorylation of Prdx1 is due to H_2O_2, activation of Src, leading Src-mediated catalytic inactivation of Prdx1 via phosphorylation.

Our data suggest that inactivation of Prdx1 via phosphorylation could be a mechanism to allow for an aberrant accumulation of H_2O_2, further promoting a carcinogenic environment and

supporting the metastatic potential of breast cancer cells. In normal circumstances, such as wound healing, a transient elevation in H_2O_2 allows the activation of wound regeneration cascades which resolve upon conclusion of wound activation, however, in the context of cancer, this is not the case[20, 27, 138].

4.0 *In vivo* prdx1 regulation of collagen architecture and extracellular matrix remodeling in the mammary gland

4.1 Introduction

The mammary gland is composed of both epithelial and stromal cells, which communicate via ECM interactions. Maintenance of tightly regulated epithelial and stromal communication is essential for normal mammary morphogenesis. Interferences with these signals can both promote and induce breast cancer progression[177]. Human breast tumors are notably stiffer than normal tissues; this characteristic has now been used to detect and classify tumor grade and invasiveness[178].

Collagen remodeling in the ECM has been well studied in the context of breast cancer. Architectural modifications of collagen fibers from curly, anisotropic orientations to linear and stiff fibers has been established as a hallmark of breast cancer aggressive potential; the mechanism behind this phenomenon, however, has yet to be fully understood[51-54, 79, 81, 179]. Collagen-I is the most abundant protein is mammals[71, 74]. Crosslinking of two α-collagen chains between triple helical domains results in the formation of pepsin-resistant β-dimers of collagen, characterized as, β11, β12 and β22[180]. Isolated crosslinked collagen β-dimers, were found to be robustly fluorescent, a phenotypic characteristic of collagen in aged tissues[180]. To date, extensive evidence has emerged implicating the ECM in governing the progression of metastases. Collagen crosslinks that are seen in remodeled stromal matrices of the tumor microenvironment provide carcinoma cells a structural scaffold promoting cancer progression[52-54, 56, 179]. Furthermore, in collagen remodeled ECM, carcinoma cells have been shown to migrate along linearized collagen fibers acting as a highway

or track, trailing behind a leading fibroblast[150]. Because activated fibroblasts are known to deposit ECM proteins such as collagen[21, 156], we hypothesized that loss of Prdx1 in stromal fibroblasts could function to promote ECM remodeling and thereby, induce cancer cell migration.

4.2 Materials and Methods

4.2.1 Syngeneic Mouse Model of Breast Cancer Metastasis

A BALB/c syngeneic mouse model was designed to evaluate tumor cell migration and ECM remodeling *in vivo*. Knockdown PRDX1 SAFs were generated through expression of 3' UTR-targeted shPrdx1. In initial studies, BALB/c SAFs (shPrdx1 or control vector) expressing iRFP were co-injected into the 4th inguinal mammary fat pad and 8-days post-injection, glands were harvested and fixed in 2% paraformaldehyde for 2 h and subsequently stored in 0.02% sodium azide-PBS solution. Following fixation, tissues were imaged using second harmonic generation (SHG) and multiphoton microscopy (MPM).

4.2.2 Second Harmonic Generation and Multiphoton Microscopy

Multiphoton microscopy with second harmonic generation on an Olympus FV1000 with multiphoton excitation (Tokyo, Japan) equipped with a Spectra-Physics DeepSee Mai Tai Ti–Sapphire laser (Newport, Mountain View, CA) with an 1.12NA 259 MPE water immersion objective was used to visualize collagen, elastin, iRFP and GFP.

4.2.3 Lentiviral shPrdx1 iRFP and GFP

Lentiviral infection of SAFs with shPrdx1 RNA was conducted as previously described in chapter 2. Infrared- red fluorescent protein (iRFP) and green fluorescent protein (GFP) were expressed into shPrdx1 SAFs via lentiviral infection. 7-days post infection, iRFP and GFP expressing SAFs were placed under hygromycin selection and subsequently expanded.

4.2.4 Collagen Quantification (*in vivo)*

Collagen deposition was quantified using ImageJ. A z-projection of 40 slices was maximally projected in an 8-bit image of the collagen only channel and locations of high tumor load (green) were quantified for collagen intensity in week 1 and week 2 injected mammary glands.

4.2.5 *In Vitro* Collagen Deposition Assay

Parental SAFs were plated in 12-well plates at a seeding density of 3 x10^4 cells per well in 10% FBS-DMEM media. Cells were incubated at 37 °C in a 5% CO_2 incubator for 6-days to allow for cellular crowding and collagen deposition. On day 6, cell layers were washed twice with 1X HBSS and collagen was extracted from cell layers via acidic porcine pepsin digestion as described previously[81, 181]. Protein samples were separated using SDS-PAGE with a 7% acrylamide resolving gel, under non-reducing conditions. Protein bands were stained using the Silver Quest kit (Invitrogen).

4.2.6 LOX Secretion

Scramble and knockdown SAFs were plated at a density of $1x10^5$ cells per 10-cm plate. Cells were serum starved in DMEM for 24 h. Following the 24 h starve, conditioned media was collected and secreted proteins were precipitated by trichloroacetic acid (TCA) precipitation as previously described[182]. Following TCA treatment, precipitates were washed twice with acetone and allowed to air dry for 10 mins. Pellets were then resuspended in 20 µl 2X Laemli sample buffer and prepared for SDS-PAGE.

4.2.7 Immunoprecipitation

HEK 293T cells (5×10^5) were transiently transfected with 2 µg pcDNA3-FLAG-LOX1 and pcDNA3-FLAG-LOXL2 plasmids, using the Fugene 6 system for 48 h. Cells were serum starved for 30 min, then treated with 100 µM H_2O_2 for 30 min. Prior to lysis, cells were washed one time with PBS containing 20 mM of NEM (N-ethylmaleimide) to avoid oxidation of free thiols. Samples were lysed using a TRIS lysis buffer (50mM Tris; 2% Triton X-100; 0.5 mM EDTA; 0.5 mM EGTA; 150 mM NaCl; 10% glycerol; 50 mM NaF; 1 mM $NaVO_4$; 40 mM β-glycerophosphate), supplemented with 30 µg/ml catalase from bovine liver (Sigma), and proteinase inhibitors. Protein concentrations were quantified using the Pierce BCA Protein Assay kit, according to the manufacturer's instructions (Thermo). 1 mg of cell lysate was incubated with 20 µL of acid treated Anti-FLAG M2 Affinity Gel (Sigma) and 400 µL lysis buffer, at 25˚ C for 3 h, with rotation. Precipitated samples were collected and washed four times with lysis buffer, and once with 1x TBS. Beads were boiled in Laemmli sample buffer (BioRad) in the presence or

absence of β-mercaptoethanol (Sigma) for 10 min. 20 µg of whole cell lysate was prepared in Laemmli sample buffer as above for 5 min.

4.3 Results

4.3.1 Extracellular Matrix Remodeling in a Syngeneic Mouse Model

To further understand the relationship between CAFs, the tumor microenvironment and breast cancer metastasis, we developed a syngeneic BALB/c mouse model. Using 8-week old female, non-parous mice, we injected iRFP expressing EV-control and iRFP-shPrdx1 SAFs into the mammary fat pad and at days 2, 4, 6 and 8 following injection, the glands were imaged using multiphoton microscopy/ second harmonic generation (MPM/SHG) microscopy (Figure 13A). MPM/SHG microscopy allows for the visualization of endogenous, repetitive structures such as collagen and elastin using second harmonic generation. Using MPM/SHG microscopy, collagen is illuminated as blue, iRFP SAFs as red and Elastin as green. In Figure 13B, a negative control, non-injected mammary gland shows typical adipose structures that are found in normal mice. On Day 2 post- injection of iRFP-EV SAFs, collagen deposition is noted, however, re-organization is not seen (Figure 13C). 2 days following injection, reorganization and deposition of collagen and elastin can be seen in glands injected with iRFP-shPrdx1 SAFs (Figure 13D). 6 days post-injection, significantly more collagen remodeling can be visualized in iRFP-shPrdx1 injected glands compared to iRFP-EV injected glands (Figure 13 E, F). To visualize migratory potential of shPrdx1 SAFs *in vivo*, images of distance travelled from injection site were compiled. iRFP-shPrdx1 SAFs migrated further away from the injection site (Figure 10H) compared to iRFP-EV

SAFs (Figure 13G). Overall, this data suggests that Prdx1 regulates ECM collagen remodeling and that loss of Prdx1 function promotes metastasis by contributing to collagen remodeling, reorganization and deposition.

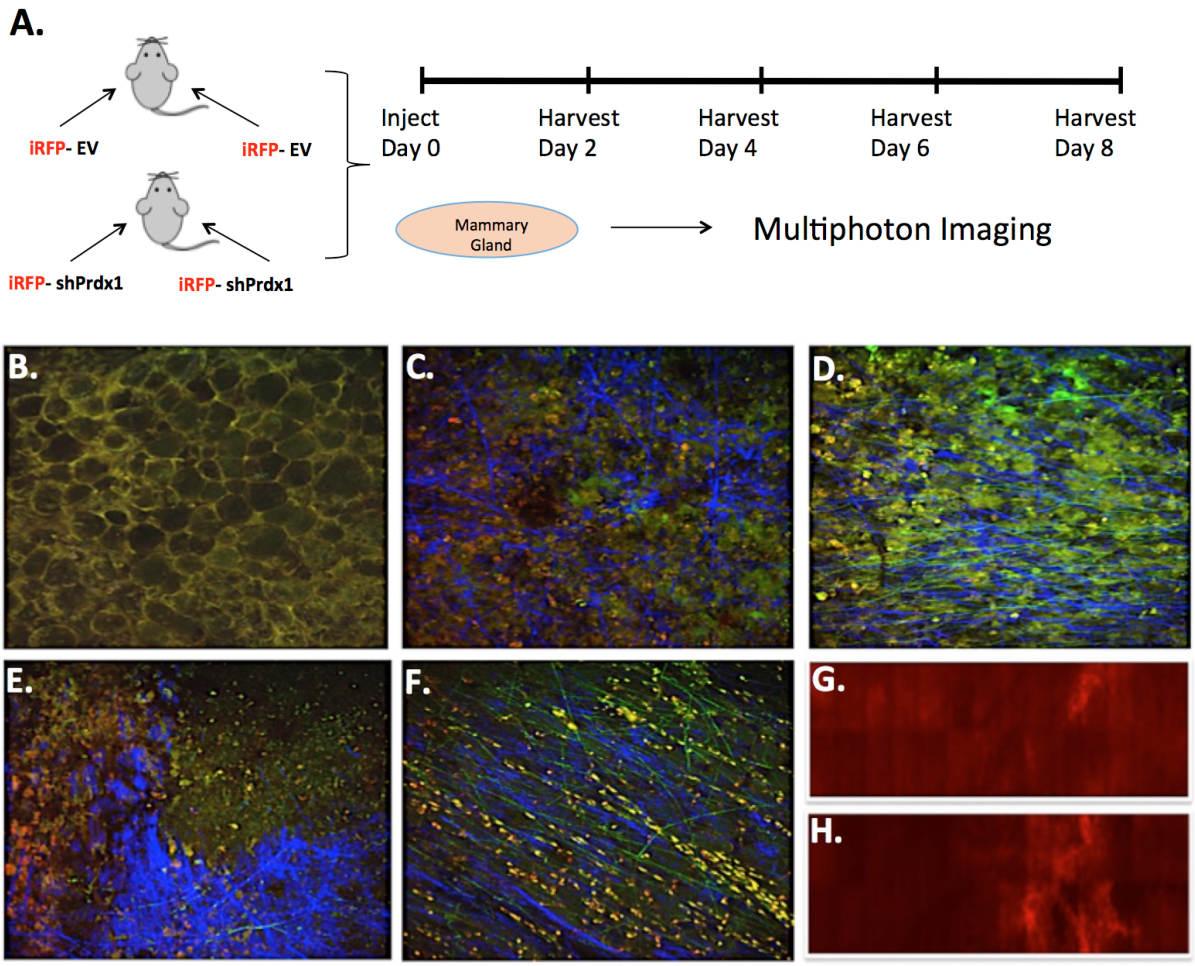

Figure 13. Loss of Prdx1 results in collagen remodeling and reorganization *in vivo* A) Schematic of syngeneic mouse model design. iRFP expressing, EV-control and shPrdx1 SAFs were injected at a density of $1x10^6$ cells into the 4^{th} inguinal mammary fat pad of BALB/c mice. Mammary glands were harvested on days 2, 4, 6 and 8 post-injection. Mammary glands were fixed in 2% PFA and prepared for MPM/SHG microscopy. B) Negative control, non-injected mammary gland showing endogenous adipose structures, C) iRFP-EV SAF injected gland, 2 days post injection, D) iRFP-shPrdx1 injected gland, 2 days post injection, E) iRFP-EV SAF injected gland, 6 days post injection, F) iRFP-shPrdx1 injected gland, 6 days post injection, G) Day 8 compiled image of SAF migration from injection site, iRFP-EV, F) iRFP-shPrdx1. Collagen=blue, Green= Elastin, Red= iRFP expressing SAFs, Yellow= Merge. N=3

4.3.2 Collagen fiber remodeling and reorganization in mammary gland

In the previous section we show data, which suggests that loss of Prdx1 in SAFs contributes to collagen and ECM remodeling. To understand if loss of Prdx1 in SAFs could contribute to breast cancer cell migration, using the same syngeneic mouse model described in section 4.3.1, we introduced a GFP expressing, non-metastatic mouse breast cancer cell line, GFP-67NR and co-injected with the iRFP expressing EV and shPrdx1 SAFs. Mammary glands were processed as described in the last section and were harvested for MPM/SHG imaging at 1-week and 2-weeks post-injection (Figure 14A). At 1 week post-injection, there was a striking difference in behavior of the GFP-67NR non-metastatic breast cancer cells. Co-injection of iRFP-EV + GFP-67NR resulted in the formation of a localized tumor surrounded by curly collagen bundles (Figure 14B). However, injection of GFP-67NR + iRFP-shPrdx1 resulted in the dispersal of the cancer cells and linearized collagen fibers (Figure 14C).

This reorganization, remodeling and cancer cell dispersion further suggested that Prdx1 is a key regulator of the tumor microenvironment. Loss of Prdx1 results in remarkable alterations in the behavior of typically non-metastatic breast cancer cells and in the structure and integrity of the stromal microenvironment. Tumoral collagen was quantified using a 40 μM z-stack of the collagen channel where there was a high localization of GFP-67NR breast cancer cells in the injected glands (Figure 15A). Tumoral collagen was significantly higher in GFP-67NR+ iRFP-shPrdx1 injected glands compared to GFP-67NR+iRFP-EV injected glands (Figure 15 B-F). Tumor-Associated Collagen Signatures (TACS) were evaluated in the MPM *in vivo* images. Although not significant, mammary glands with a co-injection of shPrdx1 SAFs and GFP67NR breast cancer cells showed a trend toward an increased TACS-3 phenotype (Figure 16).

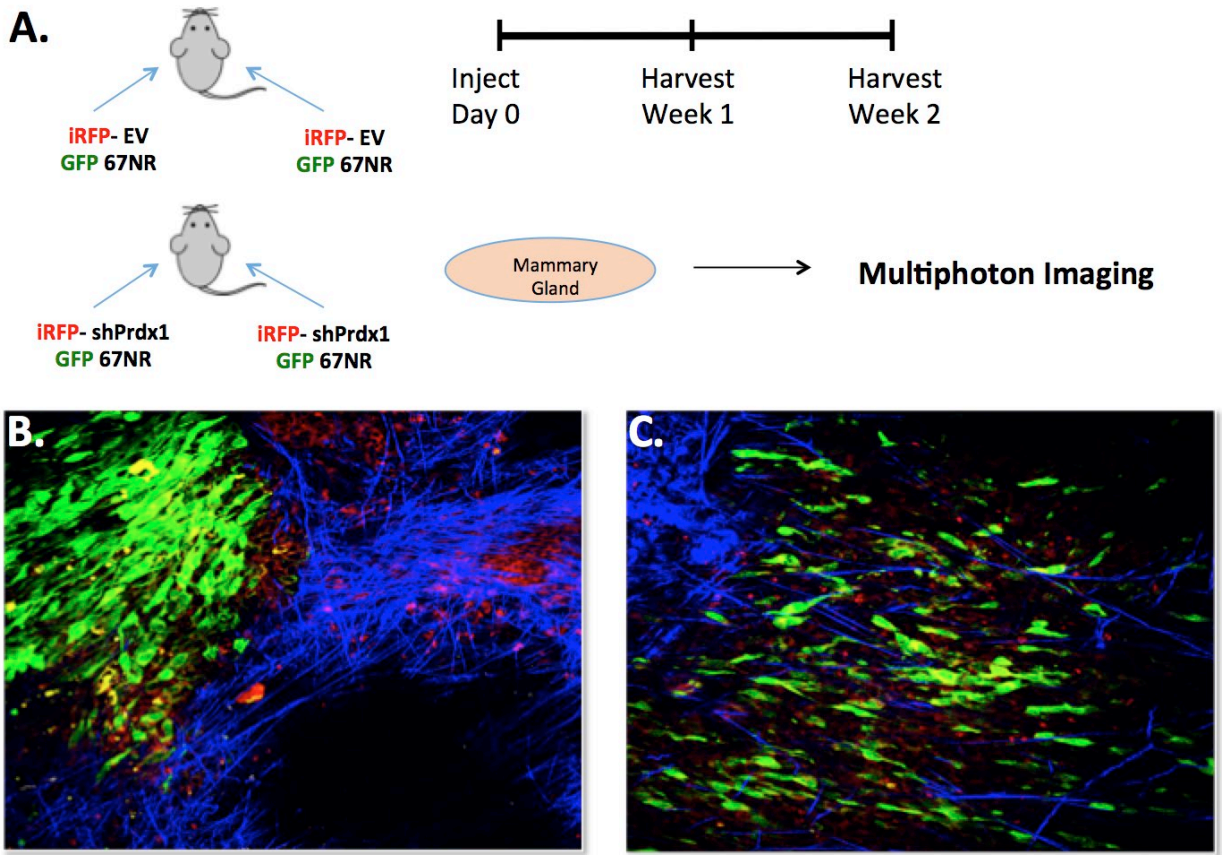

Figure 14. Loss of Prdx1 in SAFs promotes migration of non-metastatic breast cancer cells and ECM remodeling. A) Syngeneic mouse model, co-injection of GFP-67NR and iRFP-EV/iRFP-shPrdx1 SAFs into the 4th inguinal mammary fat pad. Glands were harvested at 1-week and 2-weeks and were processed for MPM/SHG imaging. B) 1-week post injection, iRFP-EV + GFP-67NR injected glands resulted in localized tumor formation surrounded by curl, relaxed collagen bundles. C). 1-week post injection, iRFP-shPrdx1 + GFP-67NR injected glands resulted in migration of GFP-67NR breast cancer cells and remodeling of the microenvironment to linearized collagen fibers. N=3

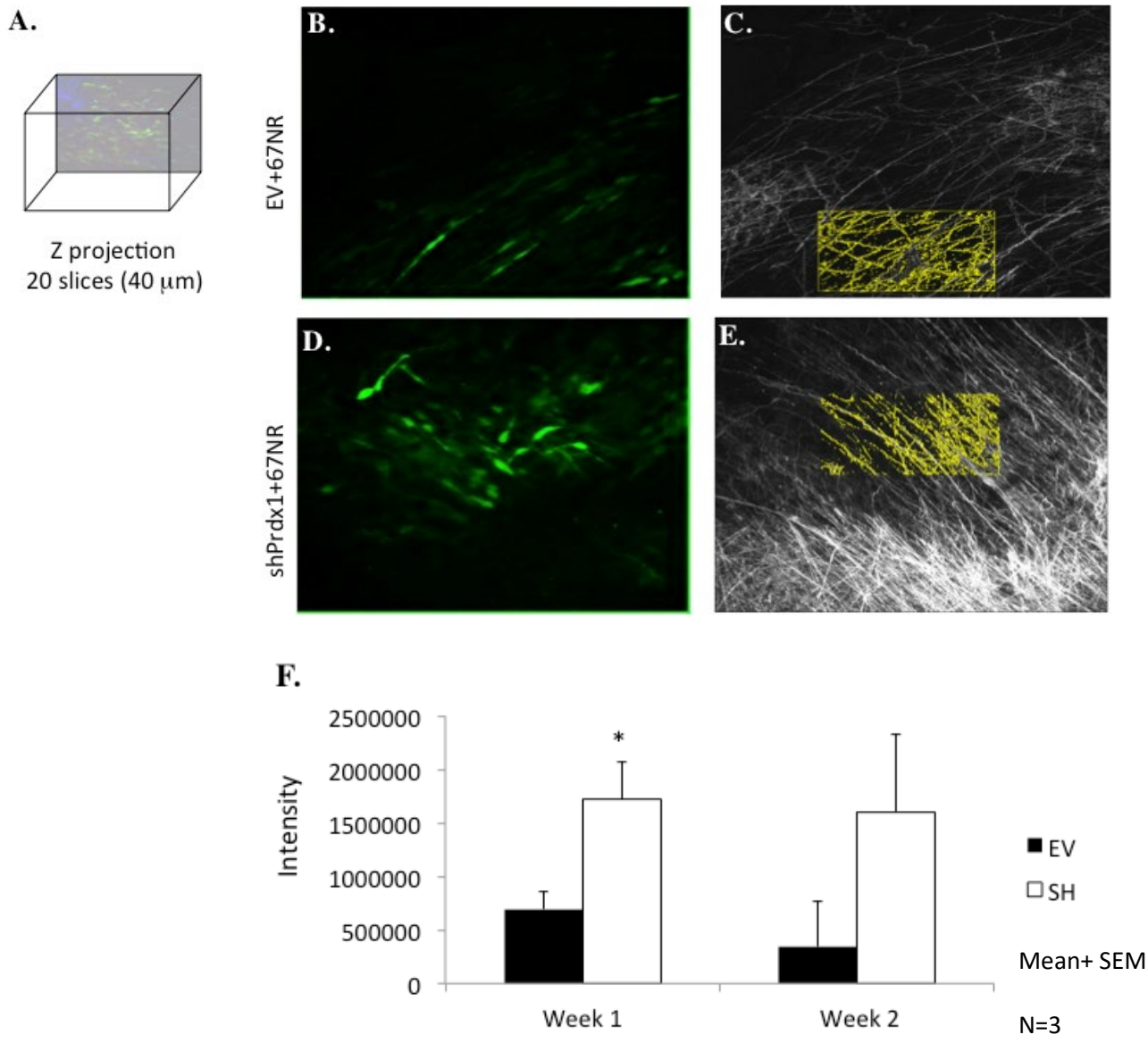

Figure 15. Quantification of tumoral collagen deposition A) z-projection of 40 slices was quantified for collagen deposition, B) Green indicates areas of high localization of GFP-67NR cells with iRFP-EV SAF co-injection, C) 8-bit image of only collagen channel in GFP-67NR + iRFP-EV injected glands, D) Green indicates areas of high localization of GFP-67NR cells with iRFP-shPrdx1 SAF co-injection, E) 8-bit image of only collagen channel in GFP-67NR + iRFP-shPrdx1 injected glands, F) Quantification of collagen fiber deposition. 1-week post injection of GFP-67NR+ iRFP-shPrdx1 injected glands resulted in significantly higher collagen deposited compared to GFP-67NR+iRFP-EV injected glands. Week 2 collagen deposition trended higher in GFP-67NR+ iRFP-shPrdx1, although not significant.

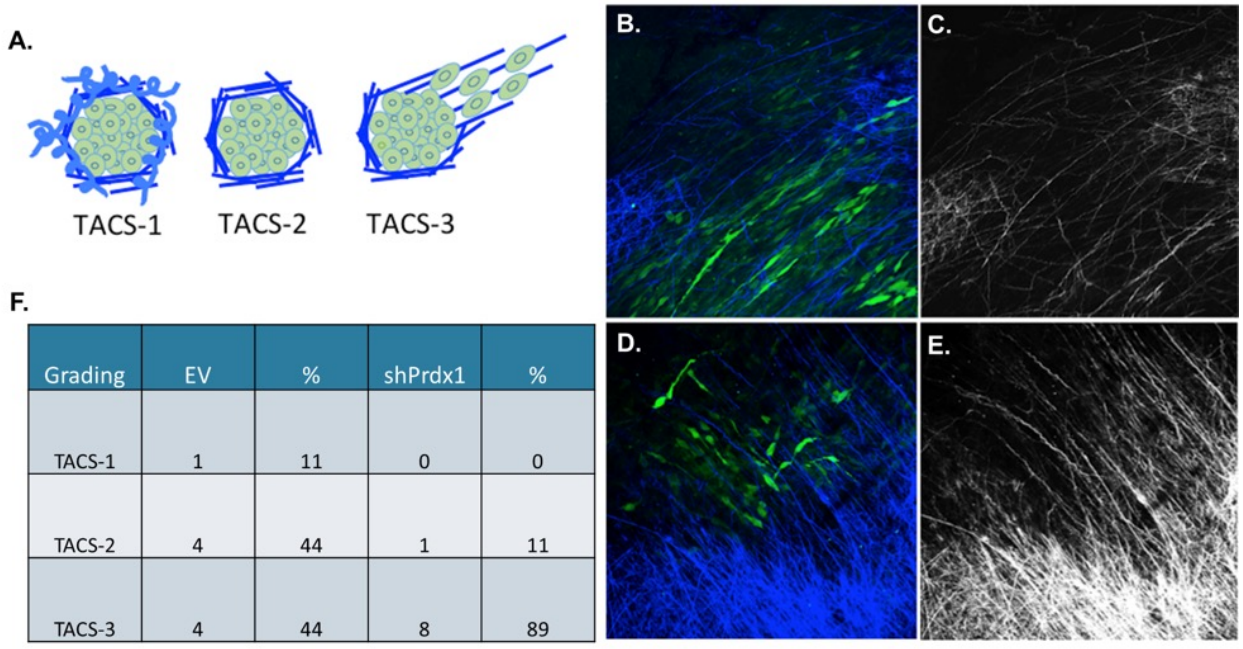

F.

Grading	EV	%	shPrdx1	%
TACS-1	1	11	0	0
TACS-2	4	44	1	11
TACS-3	4	44	8	89

Figure 16. TACS Quantification of Remodeled Collagen in Mammary Gland A) Schematic of TACS-1/TACS-2/TACS-3 characteristics, B,C) EV SAF + GFP67NR injected mammary gland 1–week post injection, collagen-only channel as 8-bit image, respectively, D,E) shPrdx1 + GFP67NR injected mammary gland 1-week post injection, collagen-only channel as 8-bit image, respectively, F) Quantification of TACS- grading by three blinded evaluators, N=3.

4.3.3 Prdx1 regulates collagen crosslinking via lysyl oxidase

Based on the *in vivo* data presented in the previous sections, we wanted to better understand the mechanism behind the remodeling of the tumor stroma that occurs when Prdx1 is absent. To address this question, we plated Scramble, shPrdx1#2 and shPrdx1#4 SAFs and allowed them to deposit collagen over a period of 6 days, we then performed a pepsin digest, ran samples on an SDS-PAGE gel and lastly stained for varying collagen bundles using silver stain (Figure 17A).

The results clearly showed that loss of Prdx1 led to increased levels of β11 and β12 crosslinked collagen as well as elevated levels of α1 and α2 non-crosslinked collagen (Figure 17B). Lysyl oxidase (LOX) is widely accepted to be the primary enzyme responsible for collagen crosslinking. To determine if the Prdx1 regulation of collagen crosslinking is dependent on LOX, we treated with βAPN, a widely used LOX inhibitor. The results clearly showed a significant reduction in β11 and β12 and a significant increase in α1 and α2 (Figure 17C). Moreover, when investigated the amount of LOX secreted from the SAFs into the ECM, it was clear that loss of Prdx1 in the shPrdx1 SAFs, resulted in a significant increase in LOX secretion compared to the Scramble control (Figure 17 D).

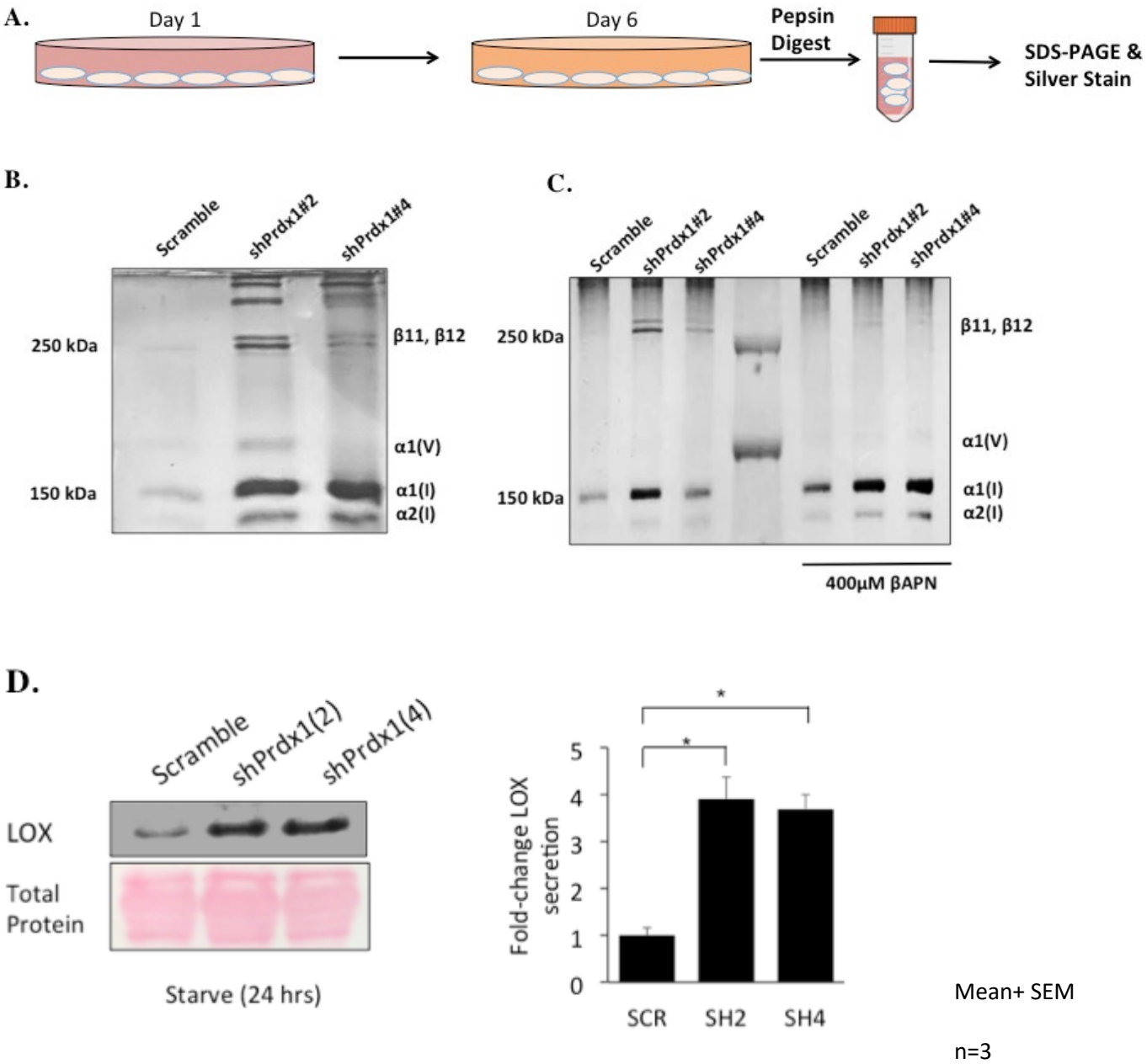

Figure 17. Prdx1 regulates LOX-dependent collagen remodeling and secretion A) Collagen deposition assay- SAFs were plated at a seeding density of 1x106 cells. Over a 6-Day period, the SAFs deposited collagen onto the plate. The cell layer was pepsin digested and subsequently run on an SDS-PAGE for silver staining. B) Loss of Prdx1 results in significant increase of β11 and β12 crosslinked collagen as well as elevated levels of α1 and α2 non-crosslinked collagen. C) Treatment with βAPN, a LOX inhibitor, resulted in a significant reduction in β11 and β12 and a significant increase in α1 and α2. D) Loss of Prdx1 also resulted in a significant increase in LOX secretion to the ECM compared to scramble control.

4.3.4 Prdx1 binds LOX and LOXL2 in a H_2O_2 -Independent Manner

Prdx1 has already been identified as a promiscuous binding partner for a wide range of signaling proteins[128]. Prdx1 is known to regulate the signaling proteins, c-Abl, c-Myc, ASK-1 and JNK via direct binding of Prdx1[174, 183-186]. However, Prdx1 regulation of collagen crosslinking enzymes such as LOX has not been previously explored. Based on the results we presented thus far, we decided to investigate whether Prdx1 directly binds to LOX, thereby regulating its function. To determine this, using 293T HEK cells we transfected FLAG-LOX and detected Prdx1-LOX binding by immunoblot. The co-immunoprecipitation results clearly showed that there was a direct binding interaction of Prdx1-LOX compared to the EV control (Figure 18A). Previous studies have established that Prdx1 binding with c-Myc and JNK can be interrupted with increasing doses of H_2O_2[187, 188]. To explore if Prdx1-LOX binding is H_2O_2-dependent, we treated the transfected FLAG-LOX samples for co-immunoprecipitation samples with 100μM H_2O_2. The results clearly indicated that PRDX1-LOX binding was not disrupted by H_2O_2 (Figure 18B). This suggested that the binding and regulation of LOX by Prdx1 was independent of H_2O_2 status. Another family of the LOXs which has been implicated in breast cancer progression is the lysyl oxidase-like 2 protein (LOXL2)[60]. Because LOX and LOXL2 have similar functions with respect to collagen crosslinking, we examined the binding interaction of Prdx1-LOXL2 with and without H_2O_2 treatment. The results, again, clearly showed that Prdx1 does directly bind to LOXL2 and it also showed that this interaction is independent of H_2O_2 concentrations (Figure 18 C, D).

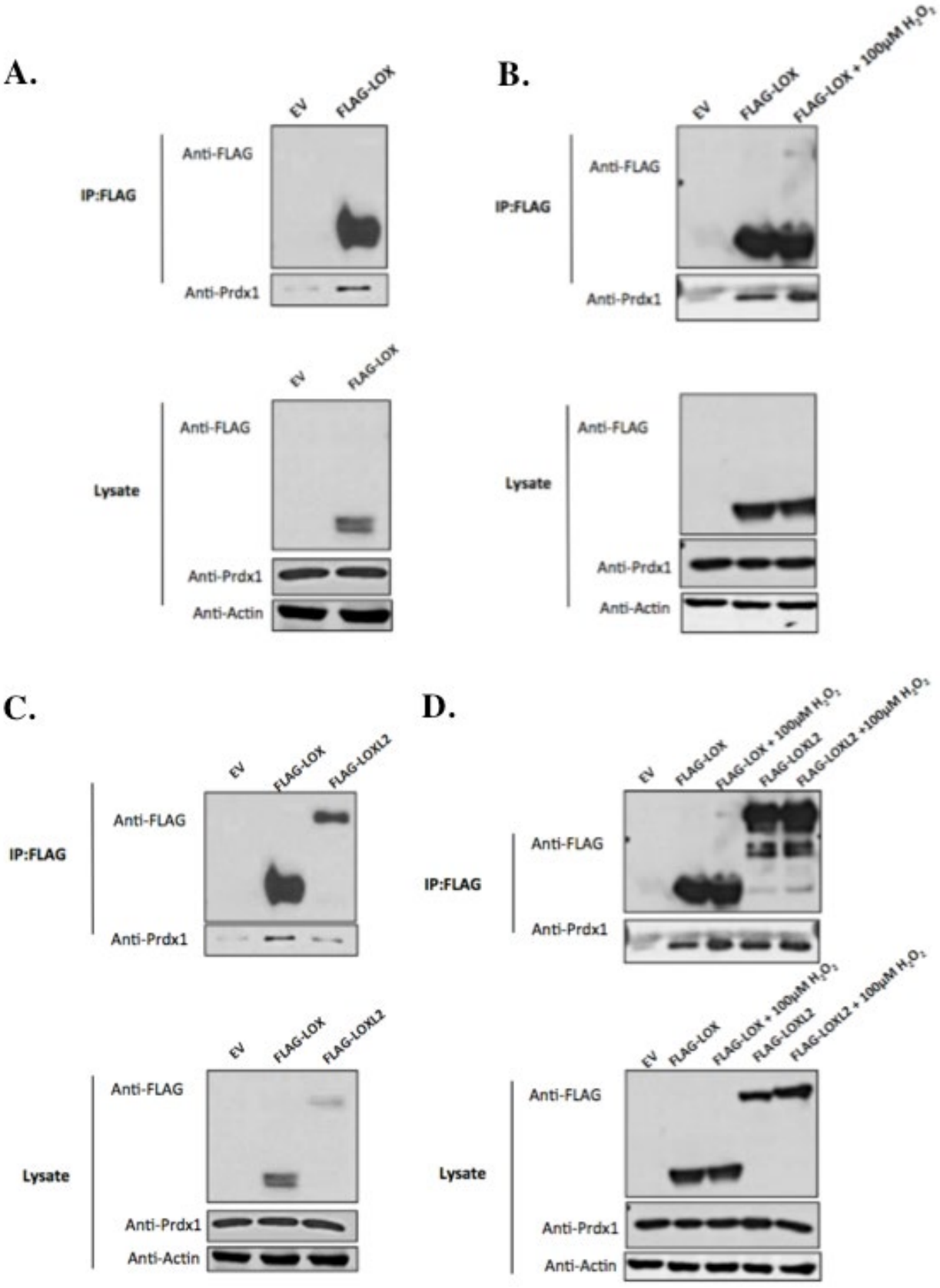
A.
EV
FLAG-LOX
IP:FLAG
Anti-FLAG
Anti-Prdx1
Lysate
Anti-FLAG
Anti-Prdx1
Anti-Actin
B.
EV
FLAG-LOX
FLAG-LOX + 100μM H2O2
IP:FLAG
Anti-FLAG
Anti-Prdx1
Lysate
Anti-FLAG
Anti-Prdx1
Anti-Actin
C.
EV
FLAG-LOX
FLAG-LOXL2
IP:FLAG
Anti-FLAG
Anti-Prdx1
Lysate
Anti-FLAG
Anti-Prdx1
Anti-Actin
D.
EV
FLAG-LOX
FLAG-LOX + 100μM H2O2
FLAG-LOXL2
FLAG-LOXL2 +100μM H2O2
IP:FLAG
Anti-FLAG
Anti-Prdx1
Lysate
Anti-FLAG
Anti-Prdx1
Anti-Actin

Figure 18. Prdx1 regulates LOX and LOXL2 via direct binding A) FLAG-LOX was transfected into 293T cells and co-immunoprecipitation was conducted. Direct binding of Prdx1-LOX was detected by immunoblot. B) FLAG-LOX binding was not interrupted by H2O2 treatment. C) Prdx1-LOXL2 co-immunoprecipitation, D) H2O2 treatment of Prdx1-LOXL2 co-immunoprecipitation. N=3

4.4 Discussion

The ECM is an invaluable regulator of tissue and cellular function in an organism and the disciplined control of its homeostasis is essential to normal functions such as wound healing and development. However, perpetual dysregulation of this homeostasis can lead to potentially fatal pathological conditions such as fibrotic disease and metastatic cancer[39, 160, 189]. Tumor development is a complex and dynamic process which involves cellular signals intrinsic to the cancer cells themselves and also extracellular, environmental cues which can significantly influence the progression of a cancer to metastasis[160, 189]. Cells with a tumorigenic phenotype have been shown to revert back to a normal phenotype by manipulation of the tumor microenvironment, suggesting that the metastatic potential of tumors is very much influenced by the ECM[163].

Architectural rearrangements of the ECM, for the most part, due to increased LOX activity has long been correlated with poor prognosis and increased metastasis and invasiveness of many cancer cell types[160]. Although ROS and ECM remodeling in the context of cancer have been well studied, the relationship between the two at the tumor-stroma interface has yet to be comprehensively studied. To address this issue, we first evaluated the role of Prdx1 in ECM remodeling *in vivo*. The results provided a striking phenotype of collagen linearization and alignment (Figure 13). This supported our hypothesis that loss of Prdx1 resulted in increased

collagen remodeling. Typically, normal stroma can function to delay and prevent tumorigenesis while aberrantly activated stroma can function to promote cancer progression[163]. Previous studies have shown that co-cultivation of stromal cells with primary breast carcinoma cells caused the tumor cells to become invasive and more migratory[163]. Furthermore, when Prdx1 levels were compared in stromal versus epithelial tissues, Prdx1were significantly higher in stromal tumor associated tissues.

To investigate if we could recapitulate this finding in the context of ROS, using a syngeneic mouse model we co-injected iRFP expressing EV/ shPrdx1 SAFs with GFP expressing 67NR breast cancer cells. 67NR breast cancer cells were selected because they are characterized as a non-aggressive and non-metastatic breast cancer cell line. Since we were examining the influence of stromal fibroblasts on cancer cell migration, we wanted to see if co-injection with shPrdx1 SAFs could indeed stimulate migration and invasion in these typically non-invasive breast cancer cells. The results of this study were again, striking. As shown in figure 14, co-injection of iRFP-shPrdx1 SAFs with GFP-67NR breast cancer cells resulted in dispersion and migration of the breast cancer cells (Figure 14C, green) with increased linearized collagen (Figure14C, blue). In control injected mammary glands, the GFP expressing 67NR breast cancer cells remained localized as a primary tumor with minimal collagen remodeling (Figure 14B). These findings further supported our hypothesis that Prdx1 had a functional role in the regulation of the ECM at the tumor stroma interface. Furthermore, for the first time, our findings provided novel evidence that stromal ECM homeostasis was partly regulated by a peroxidase, Prdx1. Moreover, when tumoral collagen was quantified, it became clear that loss of Prdx1 resulted in significantly more collagen deposition compared to the EV control (Figure 15-16).

With the findings from our *in vivo* data, we decided to first, examine if Prdx1 status could directly influence collagen crosslinking and remodeling and second, determine if LOX was the enzyme responsible for this remodeled collagen phenotype. Using the cellular crowding and collagen deposition assay, we found that loss of Prdx1 in SAFs resulted in elevated levels of β11 and β12 crosslinked collagen compared to scramble control (Figure 17B). Moreover, when treated with the LOX inhibitor, βAPN, levels of β11 and β12 crosslinked collagen decreased while non-crosslinked α1,2 levels increased (Figure 17C). It is of interest to note that typically, collagen deposition by fibroblasts is a slow process, in some cases taking over 1-month[181]. Our shPrdx1 stromal fibroblasts were able to deposit collagen matrix rapidly, taking only 6-days in the absence of any crowding agent. Furthermore, when LOX secretion was evaluated, we found that loss of Prdx1 in SAFs led to a significant increase in LOX secretion to the ECM (Figure 17D). Lastly, the direct binding of Prdx1 to LOX and LOXL2, independent of H_2O_2 status suggested that Prdx1 sequesters LOX and LOXL2 inside the cell by direct binding, preventing its secretion to the ECM (Figure18).

When exploring tumor-stroma dynamics, it's important to note that H_2O_2 is a known byproduct of LOX activity[37, 46, 58]. Previous studies have shown that removal of H_2O_2 by catalase treatment in invasive breast cancer cells resulted in loss of Src activation[58]. Moreover, when treated with βAPN, an established LOX inhibitor, Src activation was decreased[58]. This supports our hypothesis that inactivation of Prdx1 by Src activation results in ECM remodeling. In this chapter, we presented data that provides an important link between the importance of Prdx1 peroxidase activity and ECM collagen remodeling and stromal reorganization.

These data suggest and support the critical role of Prdx1 in regulating a tumor microenvironment, which is not permissive to metastasis. It has long been known that fibrotic

signals enrich tumor progression, however, the underlying mechanism behind this phenomenon is not yet fully understood. The data presented in this chapter provide novel insight into mechanisms of ECM dysregulation and collagen remodeling and place Prdx1 as a central regulator of LOX-dependent collagen remodeling in the tumor microenvironment. Our data highlight the important clinical implications for the treatment of stromal fibrosis in the tumor microenvironment and it is the first to link LOX-mediated architectural changes of the tumor ECM to a peroxidase.

5.0 General Discussion and Future Directions

Increasing evidence in the field of metastasis support the important role of the stroma and ECM in the progression of various different types of cancer. Several decades of in-depth research on breast cancer has been mostly focused on tumor cell autonomous properties. Only recently, has the field began to accept and appreciate the important role of the ECM and tumor stroma on cancer progression and metastasis. The ECM is characterized as a fertile ground for fibroblast recruitment, matrix deposition and for enhanced cancer cell-stroma communications[190].

In normal conditions, the stromal component of the ECM provides structural support and maintenance of tissue homeostasis, however, in the context of breast cancer, the stroma undergoes architectural changes via the recruitment of activated fibroblasts, enhancing aberrant stromal dynamics such an increased collagen deposition and fiber modifications. Modifications to the structure of collagen have been shown to serve as a network or highway thereby, promoting cancer cell migration[51, 52]. Although increased collagen deposition and fiber remodeling leading to elevated mammographic breast density[78] has long been correlated as a risk factor for the development of breast cancer, the mechanism behind this phenomenon was not well characterized.

The data presented in this dissertation provide novel insight into 1) understanding the functional dynamics of the tumor-stroma in relation the architectural modifications of the ECM and its significance in the context of breast cancer progression and 2) characterizing the mechanism

and key proteins involved in regulating matrix deposition and collagen remodeling via cancer-cell-stroma paracrine signaling, resulting in Prdx1 inactivation.

As described in chapters 2 and 3, Prdx1 has been established as a critical modulator of ROS homeostasis in the cytosol of the cell. Prdx1 is a peroxidase, which, when catalytically active, functions as a H_2O_2 scavenger. Most evidence in the field to date has served to classify and define Prdx1 inactivation via overoxidation of its catalytic cysteine by high doses of H_2O_2 (> 100 μM). Our initial hypothesis focused on cancer-cell secreted H_2O_2 as the mechanism by which stromal Prdx1 became inactivated. However, our initial experiments quickly confirmed that this did not occur. In fact, later experiments presented in chapter 3 showed that Prdx1 was inactivated via phosphorylation on Y194 in parental stromal fibroblasts. This was mediated by a paracrine breast cancer-cell secreted factor from MBA-MD-231breast cancer cells. Furthermore, this secreted factor was most likely either by a growth factor or H_2O_2, however, both could result in the phosphorylation and activation of SRC leading to the inactivation of Prdx1.

Inactivation of Prdx1 via phosphorylation of Y194 via an MBA-MD-231 breast cancer-cell secreted factor is a novel finding, which has not yet been observed or characterized in the field. This is of critical importance in the context of better understanding breast cancer metastasis and how early cancer cell paracrine signaling to stromal fibroblasts can lead to a cascade of events, starting with stromal Prdx1 inactivation via phosphorylation. This inactivation of Prdx1 leads to the localized accumulation of H_2O_2, which thereby suggests, that neighboring normal stromal fibroblasts can also then become activated due to further inactivation of stromal Prdx1. This positive feedback loop between MBA-MD-231 cancer-cell secreted factors suggests a mechanistic explanation of how an activated fibroblast can sustain itself without regression to basal level.

Furthermore, in this dissertation we show that sustained fibroblast activation via cancer-cell paracrine signaling leading to Prdx1 inactivation via phosphorylation, results in a cascade of ECM remodeling events, such as significantly increased collagen deposition and LOX secretion, both *in vivo* and *in vitro.* To better understand the metastatic potential of stromal Prdx1 inactivation, studies would need to be conducted *in vivo* to evaluate metastatic spread of shPrdx1 fibroblasts and breast cancer cells to distant sites in the body, such as the bone and lung, the two most common sites of breast metastases. Moreover, in terms of clinical and translational relevance, use of LOX inhibitors in combination with chemotherapy may be of value in targeting and preventing breast cancer metastases. Use of LOX inhibitors, such as tetrathiomolybdate, a potent copper chelator, in the treatment of various types of cancer, has shown limited or poor success. However, recent reports from a small phase-II clinical trial with tetrathiomolybdate, has shown that 62 of 75 patients with advanced breast cancer had no detectable evidence of disease at 5 years[191]. This further suggests that considering treatment with LOX inhibitors may be a viable therapeutic option to prevent breast cancer progression.

Appendix

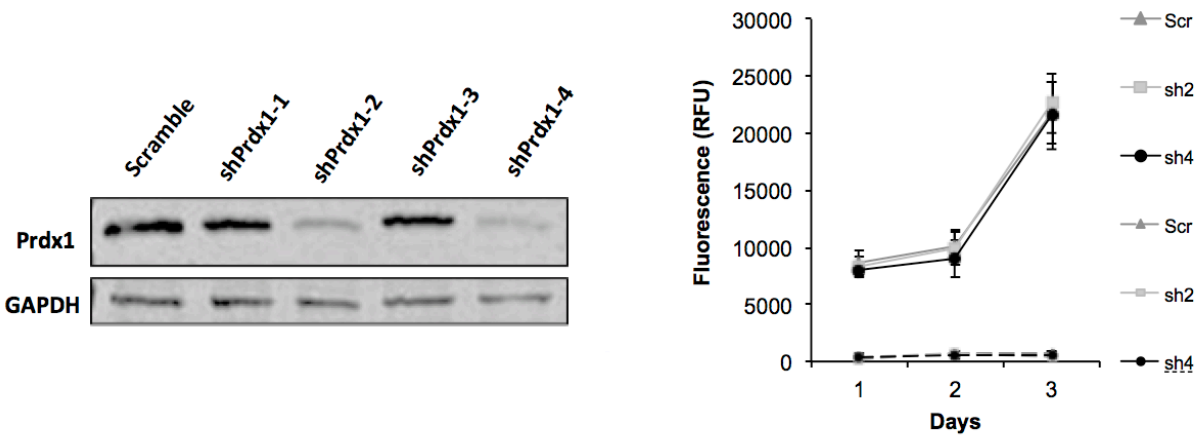

Figure 19: Supplemental Figure 1 Immunoblot of shPrdx1 knockdown constructs and protein levels and proliferation curve of scramble, shPrdx1#2 and shPrdx1#4 SAFs.

Bibliography

1. Rebecca L. Siegel MPH Kimberly D. Miller MPH Ahmedin Jemal DVM, P., Cancer statistics, 2018 - Siegel - 2018 - CA: A Cancer Journal for Clinicians - Wiley Online Library. 2018.

2. Weigelt, B.; Peterse, J. L.; Veer, L. J. v. t., Breast cancer metastasis: markers and models. Nature Reviews Cancer 2005, 5 (8), 591-602.

3. Karagiannis, G. S.; Pastoriza, J. M.; Wang, Y.; Harney, A. S.; Entenberg, D.; Pignatelli, J.; Sharma, V. P.; Xue, E. A.; Cheng, E.; D'Alfonso, T. M.; Jones, J. G.; Anampa, J.; Rohan, T. E.; Sparano, J. A.; Condeelis, J. S.; Oktay, M. H., Neoadjuvant chemotherapy induces breast cancer metastasis through a TMEM-mediated mechanism. 2017.

4. Sparano, J. A.; Gray, R. J.; Makower, D. F.; Pritchard, K. I.; Albain, K. S.; Hayes, D. F.; Charles E. Geyer, J.; Dees, E. C.; Goetz, M. P.; John A. Olson, J.; Lively, T.; Badve, S. S.; Saphner, T. J.; Wagner, L. I.; Whelan, T. J.; Ellis, M. J.; Paik, S.; Wood, W. C.; Ravdin, P. M.; Keane, M. M.; Moreno, H. L. G.; Reddy, P. S.; Goggins, T. F.; Mayer, I. A.; Brufsky, A. M.; Toppmeyer, D. L.; Kaklamani, V. G.; Berenberg, J. L.; Abrams, J.; George W. Sledge, J., Adjuvant Chemotherapy Guided by a 21-Gene Expression Assay in Breast Cancer. https://doi-org.pitt.idm.oclc.org/10.1056/NEJMoa1804710 2018.

5. Martinez, K. N. A. B. S. E., Reproductive risk factors and breast cancer subtypes: a review of the literature | SpringerLink. 2014.

6. Bredfeldt, J. S.; Liu, Y.; Conklin, M. W.; Keely, P. J.; Mackie, T. R.; Eliceiri, K. W., Automated quantification of aligned collagen for human breast carcinoma prognosis. J Pathol Inform 2014, 5, 28.

7. Shekhar, M. P.; Pauley, R.; Heppner, G., Host microenvironment in breast cancer development: Extracellular matrix–stromal cell contribution to neoplastic phenotype of epithelial cells in the breast. In Breast Cancer Res, 2003; Vol. 5, pp 130-5.

8. Yan Mao, E. T. K., David H. Garfield, Kunwei Shen, Stromal cells in tumor microenvironment and breast cancer | SpringerLink. 2012.

9. Orimo, A.; Weinberg, R. A., Stromal Fibroblasts in Cancer: A Novel Tumor-Promoting Cell Type. http://dx.doi.org.pitt.idm.oclc.org/10.4161/cc.5.15.3112 2006.

10. Whiteside, T., The tumor microenvironment and its role in promoting tumor growth. Oncogene 2008, 27 (45), 5904-12.

11. Pietras, K.; Ostman, A., Hallmarks of cancer: interactions with the tumor stroma. Exp Cell Res 2010, 316 (8), 1324-31.

12. Shiga, K.; Hara, M.; Nagasaki, T.; Sato, T.; Takahashi, H.; Takeyama, H., Cancer-Associated Fibroblasts: Their Characteristics and Their Roles in Tumor Growth. In Cancers (Basel), 2015; Vol. 7, pp 2443-58.

13. Cirri, P.; Chiarugi, P., Cancer-associated-fibroblasts and tumour cells: a diabolic liaison driving cancer progression. Cancer Metastasis Rev 2012, 31 (1-2), 195-208.

14. Ronnov-Jessen, L.; Petersen, O. W.; Bissell, M. J., Cellular changes involved in conversion of normal to malignant breast: importance of the stromal reaction. Physiol Rev 1996, 76 (1), 69-125.

15. Park, J. E.; Lenter, M. C.; Zimmermann, R. N.; Garin-Chesa, P.; Old, L. J.; Rettig, W. J., Fibroblast activation protein, a dual specificity serine protease expressed in reactive human tumor stromal fibroblasts. J Biol Chem 1999, 274 (51), 36505-12.

16. Tuxhorn, J. A.; Ayala, G. E.; Smith, M. J.; Smith, V. C.; Dang, T. D.; Rowley, D. R., Reactive Stroma in Human Prostate Cancer. 2002.

17. Virchow, R., Die Cellularpathologie in lhrer Begruendung auf Physiologische und Pathologische Gewebelehre (ed. Hirschwald, A.). Berlin, Germany, 1858.

18. Duvall, M., Atlas d'Embryologie. (ed. Masson, G.). Paris, France, 1879.

19. Kalluri, R., The biology and function of fibroblasts in cancer. Nature Reviews Cancer 2016, 16 (9), 582.

20. Kalluri, R.; Zeisberg, M., Fibroblasts in cancer. Nat Rev Cancer 2006, 6 (5), 392-401.

21. Erdogan, B.; Ao, M.; White, L. M.; Means, A. L.; Brewer, B. M.; Yang, L.; Washington, M. K.; Shi, C.; Franco, O. E.; Weaver, A. M.; Hayward, S. W.; Li, D.; Webb, D. J., Cancer-associated fibroblasts promote directional cancer cell migration by aligning fibronectin. J Cell Biol 2017, 216 (11), 3799-3816.

22. Friedl, P.; Locker, J.; Sahai, E.; Segall, J. E., Classifying collective cancer cell invasion. Nature Cell Biology 2012, 14, 777-783.

23. Sappino, A. P.; Schurch, W.; Gabbiani, G., Differentiation repertoire of fibroblastic cells: expression of cytoskeletal proteins as marker of phenotypic modulations. Lab Invest 1990, 63 (2), 144-61.

24. Gaggioli, C.; Hooper, S.; Hidalgo-Carcedo, C.; Grosse, R.; Marshall, J. F.; Harrington, K.; Sahai, E., Fibroblast-led collective invasion of carcinoma cells with differing roles for RhoGTPases in leading and following cells. Nature Cell Biology 2007, 9 (12), 1392.

25. Tao, L.; Cancer associated fibroblasts: An essential role in the tumor microenvironment (Review). Oncology Letters 2018, 14 (3), 2611-2620.

26. Buchheit, C. L.; Weigel, K. J.; Schafer, Z. T., Cancer cell survival during detachment from the ECM: multiple barriers to tumour progression. Nature Reviews Cancer 2014, 14, 632-641.

27. Flier, J. S., MD; Underhill, L. H.; Dvorak, H. F., MD, Tumors: Wounds That Do Not Heal. The New England Journal of Medicine 1986.

28. Weaver, V. M.; Petersen, O. W.; Wang, F.; Larabell, C. A.; Briand, P.; Damsky, C.; Bissell, M. J., Reversion of the Malignant Phenotype of Human Breast Cells in Three-Dimensional Culture and In Vivo by Integrin Blocking Antibodies. 1997.

29. Kenny, P. A.; Bissell, M. J., TUMOR REVERSION: CORRECTION OF MALIGNANT BEHAVIOR BY MICROENVIRONMENTAL CUES. Int J Cancer 2003, 107 (5), 688-95.

30. Ryan, G. B.; Cliff, W. J.; Gabbiani, G.; Irle, C.; Statkov, P. R.; Majno, G., Myofibroblasts in an avascular fibrous tissue. Lab Invest 1973, 29 (2), 197-206.

31. Ryan, G. B.; Cliff, W. J.; Gabbiani, G.; Irle, C.; Montandon, D.; Statkov, P. R.; Majno, G., Myofibroblasts in human granulation tissue. Human Pathology 1974, 5 (1), 55-67.

32. Löhr, M.; Schmidt, C.; Ringel, J.; Kluth, M.; Müller, P.; Nizze, H.; Jesnowski, R., Transforming Growth Factor-β1 Induces Desmoplasia in an Experimental Model of Human Pancreatic Carcinoma. **2001**.

33. Shanley, C. J.; Gharaee-Kermani, M.; Sarkar, R.; Welling, T. H.; Kriegel, A.; Ford, J. W.; Stanley, J. C.; Phan, S. H., Transforming growth factor-β1 increases lysyl oxidase enzyme activity and mRNA in rat aortic smooth muscle cells. *Journal of Vascular Surgery* **1997,** *25* (3), 446-452.

34. Qian Xiao, G. G., Lysyl Oxidase, Extracellular Matrix Remodeling and Cancer Metastasis | SpringerLink. **2012**.

35. H. A. Lucero, H. M. K., Lysyl oxidase: an oxidative enzyme and effector of cell function | SpringerLink. **2006**.

36. Kirschmann, S. L. P. M. J. C. H. D. A., Paradoxical roles for lysyl oxidases in cancer—A prospect - Payne - 2007 - Journal of Cellular Biochemistry - Wiley Online Library. *Journal of Cellular Biochemistry* **2007**.

37. Cox, T. R.; Bird, D.; Baker, A.-M.; Barker, H. E.; Ho, M. W.-Y.; Lang, G.; Erler, J. T., LOX-Mediated Collagen Crosslinking Is Responsible for Fibrosis-Enhanced Metastasis. **2013**.

38. Kirschmann, D. A.; Seftor, E. A.; Fong, S. F. T.; Nieva, D. R. C.; Sullivan, C. M.; Edwards, E. M.; Sommer, P.; Csiszar, K.; Hendrix, M. J. C., A Molecular Role for Lysyl Oxidase in Breast Cancer Invasion. **2002**.

39. Levental, K. R.; Yu, H.; Kass, L.; Lakins, J. N.; Egeblad, M.; Erler, J. T.; Fong, S. F.; Csiszar, K.; Giaccia, A.; Weninger, W.; Yamauchi, M.; Gasser, D. L.; Weaver, V. M., Matrix Crosslinking Forces Tumor Progression by Enhancing Integrin signaling. *Cell* **2009,** *139* (5), 891-906.

40. Voloshenyuk, T. G.; Landesman, E. S.; Khoutorova, E.; Hart, A. D.; Gardner, J. D., Induction of cardiac fibroblast lysyl oxidase by TGF-beta1 requires PI3K/Akt, Smad3, and MAPK signaling. *Cytokine* **2011,** *55* (1), 90-7.

41. Voloshenyuk, T. G.; Hart, A. D.; Khoutorova, E.; Gardner, J. D., TNF-alpha increases cardiac fibroblast lysyl oxidase expression through TGF-beta and PI3Kinase signaling pathways. *Biochem Biophys Res Commun* **2011,** *413* (2), 370-5.

42. Hornstra, I. K.; Birge, S.; Starcher, B.; Bailey, A. J.; Mecham, R. P.; Shapiro, S. D., Lysyl oxidase is required for vascular and diaphragmatic development in mice. *J Biol Chem* **2003,** *278* (16), 14387-93.

43. Prohaska, J. R., Genetic diseases of copper metabolism. *Clin Physiol Biochem* **1986,** *4* (1), 87-93.

44. Chanoki, M.; Ishii, M.; Kobayashi, H.; Fushida, H.; Yashiro, N.; Hamada, T.; Ooshima, A., Increased expression of lysyl oxidase in skin with scleroderma. *Br J Dermatol* **1995,** *133* (5), 710-5.

45. Murawaki, Y.; Kusakabe, Y.; Hirayama, C., Serum lysyl oxidase activity in chronic liver disease in comparison with serum levels of prolyl hydroxylase and laminin. *Hepatology* **1991,** *14* (6), 1167-73.

46. Payne, S. L.; Fogelgren, B.; Hess, A. R.; Seftor, E. A.; Wiley, E. L.; Fong, S. F. T.; Csiszar, K.; Hendrix, M. J. C.; Kirschmann, D. A., Lysyl Oxidase Regulates Breast Cancer Cell Migration and Adhesion through a Hydrogen Peroxide–Mediated Mechanism. **2005**.

47. Erler, J. T.; Bennewith, K. L.; Cox, T. R.; Lang, G.; Bird, D.; Koong, A.; Le, Q.-T.; Giaccia, A. J., Hypoxia-Induced Lysyl Oxidase Is a Critical Mediator of Bone Marrow Cell Recruitment to Form the Premetastatic Niche. *Cancer Cell* **2009,** *15* (1), 35-44.

48. Salvador, F.; Martin, A.; López-Menéndez, C.; Moreno-Bueno, G.; Santos, V.; Vázquez-Naharro, A.; Santamaria, P. G.; Morales, S.; Dubus, P. R.; Muinelo-Romay, L.; López-López, R.; Tung, J. C.; Weaver, V. M.; Portillo, F.; Cano, A., Lysyl Oxidase-like Protein LOXL2 Promotes Lung Metastasis of Breast Cancer. *Cancer Res* **2017,** *77* (21), 5846-5859.

49. Chu, I. M.; Michalowski, A. M.; Hoenerhoff, M.; Szauter, K. M.; Luger, D.; Sato, M.; Flanders, K.; Oshima, A.; Csiszar, K.; Green, J. E., GATA3 inhibits lysyl oxidase-

mediated metastases of human basal triple-negative breast cancer cells. *Oncogene* **2012,** *31* (16), 2017-27.

50. Barker, H. E.; Cox, T. R.; Erler, J. T., The rationale for targeting the LOX family in cancer. *Nat Rev Cancer* **2012,** *12* (8), 540-52.

51. Provenzano, P. P.; Inman, D. R.; Eliceiri, K. W.; Knittel, J. G.; Yan, L.; Rueden, C. T.; White, J. G.; Keely, P. J., Collagen density promotes mammary tumor initiation and progression. *BMC Medicine* **2008,** *6* (1), 11.

52. Provenzano, P. P.; Eliceiri, K. W.; Campbell, J. M.; Inman, D. R.; White, J. G.; Keely, P. J., Collagen reorganization at the tumor-stromal interface facilitates local invasion. *BMC Medicine* **2006,** *4* (1), 38.

53. Fenner, J.; Stacer, A. C.; Winterroth, F.; Johnson, T. D.; Luker, K. E.; Luker, G. D., Macroscopic Stiffness of Breast Tumors Predicts Metastasis. *Scientific Reports* **2014,** *4*.

54. Conklin, M. W.; Eickhoff, J. C.; Riching, K. M.; Pehlke, C. A.; Eliceiri, K. W.; Provenzano, P. P.; Friedl, A.; Keely, P. J., Aligned Collagen Is a Prognostic Signature for Survival in Human Breast Carcinoma. *The American Journal of Pathology* **2011,** *178* (3), 1221-1232.

55. Zhang, K.; Corsa, C. A.; Ponik, S. M.; Prior, J. L.; Piwnica-Worms, D.; Eliceiri, K. W.; Keely, P. J.; Longmore, G. D., The collagen receptor discoidin domain receptor 2 stabilizes SNAIL1 to facilitate breast cancer metastasis. *Nature Cell Biology* **2013,** *15*, 677-687.

56. Egeblad, M.; Rasch, M. G.; Weaver, V. M., Dynamic interplay between the collagen scaffold and tumor evolution. *Curr Opin Cell Biol* **2010,** *22* (5), 697-706.

57. Bondareva, A.; Downey, C. M.; Ayres, F.; Liu, W.; Boyd, S. K.; Hallgrimsson, B.; Jirik, F. R., The lysyl oxidase inhibitor, beta-aminopropionitrile, diminishes the metastatic colonization potential of circulating breast cancer cells. *PLoS One* **2009,** *4* (5), e5620.

58. Payne, S. L.; Fogelgren, B.; Hess, A. R.; Seftor, E. A.; Wiley, E. L.; Fong, S. F.; Csiszar, K.; Hendrix, M. J.; Kirschmann, D. A., Lysyl oxidase regulates breast cancer cell migration and adhesion through a hydrogen peroxide-mediated mechanism. *Cancer Res* **2005,** *65* (24), 11429-36.

59. PLOS ONE: The Lysyl Oxidase Inhibitor, Î²-Aminopropionitrile, Diminishes the Metastatic Colonization Potential of Circulating Breast Cancer Cells. http://journals.plos.org/plosone/article?id=10.1371/journal.pone.0005620.

60. Canesin, G.; Cuevas, E. P.; Santos, V.; López-Menéndez, C.; Moreno-Bueno, G.; Huang, Y.; Csiszar, K.; Portillo, F.; Peinado, H.; Lyden, D.; Cano, A., Lysyl oxidase-like 2 (LOXL2) and E47 EMT factor: novel partners in E-cadherin repression and early metastasis colonization. *Oncogene* **2014,** *0*.

61. Kim, B. R.; Dong, S. M.; Seo, S. H.; Lee, J. H.; Lee, J. M.; Lee, S. H.; Rho, S. B., Lysyl oxidase-like 2 (LOXL2) controls tumor-associated cell proliferation through the interaction with MARCKSL1. *Cell Signal* **2014,** *26* (9), 1765-73.

62. Hollosi, P.; Yakushiji, J. K.; Fong, K. S.; Csiszar, K.; Fong, S. F., Lysyl oxidase-like 2 promotes migration in noninvasive breast cancer cells but not in normal breast epithelial cells. *Int J Cancer* **2009,** *125* (2), 318-27.

63. Baker, A.-M.; Bird, D.; Lang, G.; Cox, T. R.; Erler, J. T., Lysyl oxidase enzymatic function increases stiffness to drive colorectal cancer progression through FAK. *Oncogene* **2012,** *32* (14), 1863.

64. Kim, Y.; Department of Biochemistry, S. o. M., Wonkwang University, Iksan-City, Jeollabuk-Do 570-749, Korea. youngkim@wku.ac.kr; Roh, S.; Park, J.-Y.; Kim, Y.; Cho, D. H.; Kim, J. C., Differential expression of the LOX family genes in human colorectal adenocarcinomas. *Oncology Reports* **2018,** *22* (4), 799-804.

65. Choi, J.; Chung, T.; Rhee, H.; Kim, Y. J.; Jeon, Y.; Yoo, J. E.; Noh, S.; Han, D. H.; Park, Y. N., Increased Expression of the Matrix-Modifying Enzyme Lysyl Oxidase-Like 2 in Aggressive Hepatocellular Carcinoma with Poor Prognosis. *Gut Liver* **2018**.

66. Bouez, C.; Reynaud, C.; Noblesse, E.; Thépot, A.; Gleyzal, C.; Kanitakis, J.; Perrier, E.; Damour, O.; Sommer, P., The Lysyl Oxidase LOX Is Absent in Basal and Squamous Cell Carcinomas and Its Knockdown Induces an Invading Phenotype in a Skin Equivalent Model. **2006**.

67. Park, J. S.; Lee, J.; Lee, Y. S.; Kim, J. K.; Dong, S. M.; Yoon, D. S., Emerging role of LOXL2 in the promotion of pancreas cancer metastasis. In *Oncotarget*, 2016; Vol. 7, pp 42539-52.

68. Tanaka, N.; Yamada, S.; Sonohara, F.; Suenaga, M.; Hayashi, M.; Takami, H.; Niwa, Y.; Hattori, N.; Iwata, N.; Kanda, M.; Tanaka, C.; Kobayashi, D.; Nakayama, G.; Koike, M.; Fujiwara, M.; Fujii, T.; Kodera, Y., Clinical Implications of Lysyl Oxidase-Like Protein 2 Expression in Pancreatic Cancer. *Scientific Reports* **2018,** *8* (1), 9846.

69. Peinado, H.; Moreno-Bueno, G.; Hardisson, D.; Pérez-Gómez, E.; Santos, V.; Mendiola, M.; Diego, J. I. d.; Nistal, M.; Quintanilla, M.; Portillo, F.; Cano, A., Lysyl Oxidase–Like 2 as a New Poor Prognosis Marker of Squamous Cell Carcinomas. **2008**.

70. Myllyharju, J.; Kivirikko, K. I., Collagens, modifying enzymes and their mutations in humans, flies and worms. *Trends Genet* **2004,** *20* (1), 33-43.

71. Shoulders, M. D.; Raines, R. T., Collagen structure and stability. *Annu Rev Biochem* **2009,** *78*, 929-58.

72. Kalluri, R., Basement membranes: structure, assembly and role in tumour angiogenesis. *Nat Rev Cancer* **2003,** *3* (6), 422-33.

73. Brodsky, B.; Persikov, A. V., Molecular structure of the collagen triple helix. *Adv Protein Chem* **2005,** *70*, 301-39.

74. Kadler, K. E.; Baldock, C.; Bella, J.; Boot-Handford, R. P., Collagens at a glance. **2007**.

75. Rowe, R. G.; Weiss, S. J., Breaching the basement membrane: who, when and how? *Trends Cell Biol* **2008,** *18* (11), 560-74.

76. Paszek, M. J.; Weaver, V. M., The tension mounts: mechanics meets morphogenesis and malignancy. *J Mammary Gland Biol Neoplasia* **2004,** *9* (4), 325-42.

77. Paszek, M. J.; Zahir, N.; Johnson, K. R.; Lakins, J. N.; Rozenberg, G. I.; Gefen, A.; Reinhart-King, C. A.; Margulies, S. S.; Dembo, M.; Boettiger, D.; Hammer, D. A.; Weaver, V. M., Tensional homeostasis and the malignant phenotype. *Cancer Cell* **2005,** *8* (3), 241-54.

78. Wolfe, J. N., Risk for breast cancer development determined by mammographic parenchymal pattern. *Cancer* **1976,** *37* (5), 2486-92.

79. Fang, M.; Yuan, J.; Peng, C.; Li, Y., Collagen as a double-edged sword in tumor progression. In *Tumour Biol*, 2014; Vol. 35, pp 2871-82.

80. Wyckoff, J. B.; Wang, Y.; Lin, E. Y.; Li, J. F.; Goswami, S.; Stanley, E. R.; Segall, J. E.; Pollard, J. W.; Condeelis, J., Direct visualization of macrophage-assisted tumor cell intravasation in mammary tumors. *Cancer Res* **2007,** *67* (6), 2649-56.

81. Lareu, R. R.; The biological relevance of the excluded volume effect. *FEBS Letters* **2017,** *581* (14), 2709-2714.

82. Margreet C M Vissers, M. H., Anthony J. Kettle, *Hydrogen Peroxide Metabolism in Health and Disease*. 2017.

83. Sies, H., Hydrogen peroxide as a central redox signaling molecule in physiological oxidative stress: Oxidative eustress. *Redox Biol* **2017,** *11*, 613-619.

84. Stone, J. R.; Yang, S., Hydrogen peroxide: a signaling messenger. *Antioxid Redox Signal* **2006,** *8* (3-4), 243-70.

85. Boveris, A.; Oshino, N.; Chance, B., The cellular production of hydrogen peroxide. *Biochem J* **1972,** *128* (3), 617-30.

86. St-Pierre, J.; Buckingham, J. A.; Roebuck, S. J.; Brand, M. D., Topology of superoxide production from different sites in the mitochondrial electron transport chain. *J Biol Chem* **2002,** *277* (47), 44784-90.

87. Murphy, M. P., How mitochondria produce reactive oxygen species. *Biochem J* **2009,** *417* (1), 1-13.

88. Kussmaul, L.; Hirst, J., The mechanism of superoxide production by NADH:ubiquinone oxidoreductase (complex I) from bovine heart mitochondria. *Proc Natl Acad Sci U S A* **2006,** *103* (20), 7607-12.

89. Kudin, A. P.; Bimpong-Buta, N. Y.; Vielhaber, S.; Elger, C. E.; Kunz, W. S., Characterization of superoxide-producing sites in isolated brain mitochondria. *J Biol Chem* **2004,** *279* (6), 4127-35.

90. Cadenas, E.; Boveris, A.; Ragan, C. I.; Stoppani, A. O., Production of superoxide radicals and hydrogen peroxide by NADH-ubiquinone reductase and ubiquinol-cytochrome c reductase from beef-heart mitochondria. *Arch Biochem Biophys* **1977,** *180* (2), 248-57.

91. Loschen, G.; Azzi, A.; Richter, C.; Flohe, L., Superoxide radicals as precursors of mitochondrial hydrogen peroxide. *FEBS Lett* **1974,** *42* (1), 68-72.

92. Weisiger, R. A.; Fridovich, I., Superoxide dismutase. Organelle specificity. *J Biol Chem* **1973,** *248* (10), 3582-92.

93. Chance, B.; Sies, H.; Boveris, A., Hydroperoxide metabolism in mammalian organs. *Physiol Rev* **1979,** *59* (3), 527-605.

94. Tyler, D. D., Polarographic assay and intracellular distribution of superoxide dismutase in rat liver. *Biochem J* **1975,** *147* (3), 493-504.

95. Antonenkov, V. D.; Grunau, S.; Ohlmeier, S.; Hiltunen, J. K., Peroxisomes are oxidative organelles. *Antioxid Redox Signal* **2010,** *13* (4), 525-37.

96. Margittai, E.; Low, P.; Stiller, I.; Greco, A.; Garcia-Manteiga, J. M.; Pengo, N.; Benedetti, A.; Sitia, R.; Banhegyi, G., Production of H(2)O(2) in the endoplasmic reticulum promotes in vivo disulfide bond formation. *Antioxid Redox Signal* **2012,** *16* (10), 1088-99.

97. Nohl, H.; Gille, L., Lysosomal ROS formation. *Redox Rep* **2005,** *10* (4), 199-205.

98. Babior, B. M., NADPH oxidase: an update. *Blood* **1999,** *93* (5), 1464-76.

99. Hernanz, R.; Briones, A. M.; Salaices, M.; Alonso, M. J., New roles for old pathways? A circuitous relationship between reactive oxygen species and cyclo-oxygenase in hypertension. *Clin Sci (Lond)* **2014,** *126* (2), 111-21.

100. Cho, K. J.; Seo, J. M.; Kim, J. H., Bioactive lipoxygenase metabolites stimulation of NADPH oxidases and reactive oxygen species. *Mol Cells* **2011,** *32* (1), 1-5.

101. Kelley, E. E.; Khoo, N. K.; Hundley, N. J.; Malik, U. Z.; Freeman, B. A.; Tarpey, M. M., Hydrogen peroxide is the major oxidant product of xanthine oxidase. *Free Radic Biol Med* **2010,** *48* (4), 493-8.

102. Valko, M.; Rhodes, C. J.; Moncol, J.; Izakovic, M.; Mazur, M., Free radicals, metals and antioxidants in oxidative stress-induced cancer. *Chem Biol Interact* **2006,** *160* (1), 1-40.

103. Mueller, S., Sensitive and nonenzymatic measurement of hydrogen peroxide in biological systems. *Free Radic Biol Med* **2000,** *29* (5), 410-5.

104. Ho, Y. S.; Xiong, Y.; Ma, W.; Spector, A.; Ho, D. S., Mice lacking catalase develop normally but show differential sensitivity to oxidant tissue injury. *J Biol Chem* **2004,** *279* (31), 32804-12.

105. Ho, Y. S.; Magnenat, J. L.; Bronson, R. T.; Cao, J.; Gargano, M.; Sugawara, M.; Funk, C. D., Mice deficient in cellular glutathione peroxidase develop normally and show no increased sensitivity to hyperoxia. *J Biol Chem* **1997,** *272* (26), 16644-51.

106. Neumann, C. A.; Krause, D. S.; Carman, C. V.; Das, S.; Dubey, D. P.; Abraham, J. L.; Bronson, R. T.; Fujiwara, Y.; Orkin, S. H.; Van Etten, R. A., Essential role for the peroxiredoxin Prdx1 in erythrocyte antioxidant defence and tumour suppression. *Nature* **2003,** *424* (6948), 561-5.

107. Wong, C. M.; Zhou, Y.; Ng, R. W.; Kung Hf, H. F.; Jin, D. Y., Cooperation of yeast peroxiredoxins Tsa1p and Tsa2p in the cellular defense against oxidative and nitrosative stress. *J Biol Chem* **2002,** *277* (7), 5385-94.

108. Wong, C. M.; Siu, K. L.; Jin, D. Y., Peroxiredoxin-null yeast cells are hypersensitive to oxidative stress and are genomically unstable. *J Biol Chem* **2004,** *279* (22), 23207-13.

109. Kirkman, H. N.; Gaetani, G. F., Mammalian catalase: a venerable enzyme with new mysteries. *Trends Biochem Sci* **2007,** *32* (1), 44-50.

110. Switala, J.; Loewen, P. C., Diversity of properties among catalases. *Arch Biochem Biophys* **2002,** *401* (2), 145-54.

111. Epp, O.; Ladenstein, R.; Wendel, A., The refined structure of the selenoenzyme glutathione peroxidase at 0.2-nm resolution. *Eur J Biochem* **1983,** *133* (1), 51-69.

112. Brigelius-Flohé R 1 , M. M., Glutathione peroxidases. Biochim Biophys Acta. : 2013.

113. Wood, Z. A.; Poole, L. B.; Karplus, P. A., Peroxiredoxin Evolution and the Regulation of Hydrogen Peroxide Signaling. **2003**.

114. Kang SW 1 , C. H., Seo MS , Kim K , Baines IC , Rhee SG . Mammalian peroxiredoxin isoforms can reduce hydrogen peroxide generated in response to growth factors and tumor necrosis factor-alpha. J Biol Chem. : 1998.

115. Peskin, A. V.; Low, F. M.; Paton, L. N.; Maghzal, G. J.; Hampton, M. B.; Winterbourn, C. C., The high reactivity of peroxiredoxin 2 with H(2)O(2) is not reflected in its reaction with other oxidants and thiol reagents. *J Biol Chem* **2007,** *282* (16), 11885-92.

116. Copley, S. D.; Novak, W. R.; Babbitt, P. C., Divergence of function in the thioredoxin fold suprafamily: evidence for evolution of peroxiredoxins from a thioredoxin-like ancestor. *Biochemistry* **2004,** *43* (44), 13981-95.

117. Hall, A.; Nelson, K.; Poole, L. B.; Karplus, P. A., Structure-based insights into the catalytic power and conformational dexterity of peroxiredoxins. *Antioxid Redox Signal* **2011,** *15* (3), 795-815.

118. Chae, H. Z.; Uhm, T. B.; Rhee, S. G., Dimerization of thiol-specific antioxidant and the essential role of cysteine 47. *Proc Natl Acad Sci U S A* **1994,** *91* (15), 7022-6.

119. Kim, S. G. R. S. W. K. T. S. C. W. J. K., Peroxiredoxin, a Novel Family of Peroxidases - Rhee - 2001 - IUBMB Life - Wiley Online Library. *IUBMB* **2008**.

120. Wood, Z. A.; Poole, L. B.; Hantgan, R. R.; Karplus, P. A., Dimers to doughnuts: redox-sensitive oligomerization of 2-cysteine peroxiredoxins. *Biochemistry* **2002,** *41* (17), 5493-504.

121. Guimaraes, B. G.; Souchon, H.; Honore, N.; Saint-Joanis, B.; Brosch, R.; Shepard, W.; Cole, S. T.; Alzari, P. M., Structure and mechanism of the alkyl hydroperoxidase AhpC, a key element of the Mycobacterium tuberculosis defense system against oxidative stress. *J Biol Chem* **2005,** *280* (27), 25735-42.

122. Peskin, A. V.; Dickerhof, N.; Poynton, R. A.; Paton, L. N.; Pace, P. E.; Hampton, M. B.; Winterbourn, C. C., Hyperoxidation of peroxiredoxins 2 and 3: rate constants for the reactions of the sulfenic acid of the peroxidatic cysteine. *J Biol Chem* **2013,** *288* (20), 14170-7.

123. Lowther, W. T.; Haynes, A. C., Reduction of cysteine sulfinic acid in eukaryotic, typical 2-Cys peroxiredoxins by sulfiredoxin. *Antioxid Redox Signal* **2011,** *15* (1), 99-109.

124. Peskin, A. V.; Pace, P. E.; Behring, J. B.; Paton, L. N.; Soethoudt, M.; Bachschmid, M. M.; Winterbourn, C. C., Glutathionylation of the Active Site Cysteines of Peroxiredoxin 2 and Recycling by Glutaredoxin. *J Biol Chem* **2016,** *291* (6), 3053-62.

125. Declercq, J. P.; Evrard, C.; Clippe, A.; Stricht, D. V.; Bernard, A.; Knoops, B., Crystal structure of human peroxiredoxin 5, a novel type of mammalian peroxiredoxin at 1.5 A resolution. *J Mol Biol* **2001,** *311* (4), 751-9.

126. Knoops, B.; Goemaere, J.; Van der Eecken, V.; Declercq, J. P., Peroxiredoxin 5: structure, mechanism, and function of the mammalian atypical 2-Cys peroxiredoxin. *Antioxid Redox Signal* **2011,** *15* (3), 817-29.

127. Fisher, A. B., Peroxiredoxin 6: a bifunctional enzyme with glutathione peroxidase and phospholipase A(2) activities. *Antioxid Redox Signal* **2011,** *15* (3), 831-44.

128. A., N. C.; Cao, J.; Manevich, Y., Peroxiredoxin 1 and its role in cell signaling. *http://dx.doi.org.pitt.idm.oclc.org/10.4161/cc.8.24.10242* **2009**.

129. Sobotta, M. C.; Liou, W.; Stocker, S.; Talwar, D.; Oehler, M.; Ruppert, T.; Scharf, A. N.; Dick, T. P., Peroxiredoxin-2 and STAT3 form a redox relay for H2O2 signaling. *Nat Chem Biol* **2015,** *11* (1), 64-70.

130. Jarvis, R. M.; Hughes, S. M.; Ledgerwood, E. C., Peroxiredoxin 1 functions as a signal peroxidase to receive, transduce, and transmit peroxide signals in mammalian cells. *Free Radic Biol Med* **2012,** *53* (7), 1522-30.

131. Stocker, S.; Maurer, M.; Ruppert, T.; Dick, T. P., A role for 2-Cys peroxiredoxins in facilitating cytosolic protein thiol oxidation. *Nat Chem Biol* **2018,** *14* (2), 148-155.

132. Tavender, T. J.; Springate, J. J.; Bulleid, N. J., Recycling of peroxiredoxin IV provides a novel pathway for disulphide formation in the endoplasmic reticulum. *Embo j* **2010,** *29* (24), 4185-97.

133. Wei, P. C.; Hsieh, Y. H.; Su, M. I.; Jiang, X.; Hsu, P. H.; Lo, W. T.; Weng, J. Y.; Jeng, Y. M.; Wang, J. M.; Chen, P. L.; Chang, Y. C.; Lee, K. F.; Tsai, M. D.; Shew, J. Y.; Lee, W. H., Loss of the oxidative stress sensor NPGPx compromises GRP78 chaperone activity and induces systemic disease. *Mol Cell* **2012,** *48* (5), 747-59.

134. Brigelius-Flohe, R.; Flohe, L., Basic principles and emerging concepts in the redox control of transcription factors. *Antioxid Redox Signal* **2011,** *15* (8), 2335-81.